SoftwareX 13 (2021) 100658

Contents lists available at ScienceDirect

SoftwareX

journal homepage: www.elsevier.com/locate/softx

Original software publication

Open data from the first and second observing runs of Advanced LIGO and Advanced Virgo

Rich Abbott [1], Thomas D. Abbott [2], Sheelu Abraham [3], Fausto Acernese [4,5], Kendall Ackley [6], Carl Adams [7], Rana X. Adhikari [1], Vaishali B. Adya [8], Christoph Affeldt [9,10], Michalis Agathos [11,12], Kazuhiro Agatsuma [13], Nancy Aggarwal [14], Odylio D. Aguiar [15], Amit Aich [16], Lorenzo Aiello [17,18], Anirban Ain [3], Ajith Parameswaran [19], Gabrielle Allen [20], Annalisa Allocca [21], Paul A. Altin [8], Alex Amato [22], Shreya Anand [1], Alena Ananyeva [1], Stuart B. Anderson [1], Warren G. Anderson [23], Svetoslava V. Angelova [24], Stefano Ansoldi [25,26], Sarah Antier [27], Stephen Appert [1], Koji Arai [1], Melody C. Araya [1], Joseph S. Areeda [28], Marc Arène [27], Nicolas Arnaud [29,30], Scott M. Aronson [31], Kg G. Arun [32], Stefano Ascenzi [17,33], Gregory Ashton [6], Stuart M. Aston [7], Pia Astone [34], Florian Aubin [35], Peter Aufmuth [10], Kellie AultONeal [36], Corey Austin [2], Valerie Avendano [37], Stanislav Babak [27], Philippe Bacon [27], Francesca Badaracco [17,18], Maria K.M. Bader [38], Sangwook Bae [39], Anne M. Baer [40], Jonathon Baird [27], Francesca Baldaccini [41,42], Giulio Ballardin [30], Stefan W. Ballmer [43], Anna-marie Bals [36], Alexander Balsamo [40], Gregory Baltus [44], Sharan Banagiri [45], Deepak Bankar [3], Rameshwar S. Bankar [3], Juan C. Barayoga [1], Claudio Barbieri [46,47], Barry C. Barish [1], David Barker [48], Kevin Barkett [49], Pablo Barneo [50], Fabrizio Barone [51,5], Bryan Barr [52], Lisa Barsotti [53], Matteo Barsuglia [27], Daniel Barta [54], Jeffrey Bartlett [48], Imre Bartos [31], Riccardo Bassiri [55], Andrea Basti [56,21], Mateusz Bawaj [57,42], Joseph C. Bayley [52], Marco Bazzan [58,59], Bence Bécsy [60], Michal Bejger [61], Imene Belahcene [29], Angus S. Bell [52], Deeksha Beniwal [62], Michael G. Benjamin [36], Joe D. Bentley [13], Fabio Bergamin [9], Beverly K. Berger [55], Gerald Bergmann [9,10], Sebastiano Bernuzzi [11], Christopher P.L. Berry [14], Diego Bersanetti [63], Alessandro Bertolini [38], Joseph Betzwieser [7], Rohan Bhandare [64], Ankit V. Bhandari [3], Jeffrey Bidler [28], Edward Biggs [23], Igor A. Bilenko [65], Garilynn Billingsley [1], Ross Birney [66], Ofek Birnholtz [67,68], Sebastien Biscans [1,53], Matteo Bischi [69,70], Sylvia Biscoveanu [53], Aparna Bisht [10], Guldauren Bissenbayeva [16], Massimiliano Bitossi [30,21], Marieanne A. Bizouard [71], Kent K. Blackburn [1], Jonathan Blackman [49], Carl D. Blair [7], David G. Blair [72], Ryan M. Blair [48], Fabrizio Bobba [73,74], Nina Bode [9,10], Michel Boer [71], Yannick Boetzel [75], Gilles Bogaert [71], Francois Bondu [76], Edgard Bonilla [55], Romain Bonnand [35], Phillip Booker [9,10], Boris A. Boom [38], Rolf Bork [1], Valerio Boschi [21], Sukanta Bose [3], Vladimir Bossilkov [72], Joel Bosveld [72], Yann Bouffanais [58,59], Antonella Bozzi [30], Carlo Bradaschia [21], Patrick R. Brady [23], Alyssa Bramley [7], Marica Branchesi [17,18], Jim E. Brau [77], Matteo Breschi [11], Tristan Briant [78], Joseph H. Briggs [52], Francesco Brighenti [69,70], Alain Brillet [71], Marc Brinkmann [9,10], Patrick Brockill [23], Aidan F. Brooks [1], Jonathan Brooks [30], Daniel D. Brown [62], Sharon Brunett [1], Giacomo Bruno [79], Robert Bruntz [40], Aaron Buikema [53], Tomasz Bulik [80], Henk J. Bulten [81,38], Alessandra Buonanno [82,83], Damir Buskulic [35], Robert L. Byer [55],

E-mail addresses: lsc-spokesperson@ligo.org, virgo-spokesperson@ego-gw.it.

https://doi.org/10.1016/j.softx.2021.100658

Miriam Cabero [9,10], Laura Cadonati [84], Giampietro Cagnoli [85], Craig Cahillane [1], Juan Calderón Bustillo [6], Jack D. Callaghan [52], Thomas A. Callister [1], Enrico Calloni [86,5], Jordan B. Camp [87], Maurizio Canepa [88,63], Kipp C. Cannon [89], Huy-tuong Cao [62], Junwei Cao [90], Giovanni Carapella [73,74], Franco Carbognani [30], Santiago Caride [91], Matthew F. Carney [14], Gregorio Carullo [56,21], Julia Casanueva Diaz [21], Claudio Casentini [92,33], Javier Castañeda [50], Sarah Caudill [38], Marco Cavaglià [93], Fabien Cavalier [29], Roberto Cavalieri [30], Giancarlo Cella [21], Pablo Cerdá-Durán [94], Elisabetta Cesarini [95,33], Oualid Chaibi [71], Kabir Chakravarti [3], Chiwai Chan [89], Manleong Chan [52], Shiuh Chao [96], Philip Charlton [97], Eve A. Chase [14], Eric Chassande-Mottin [27], Deep Chatterjee [23], Mayank Chaturvedi [64], Hsin-yu Y. Chen [100], Xu Chen [72], Yanbei Chen [49], Hai-ping Cheng [31], Chi-kit K. Cheong [101], Hanyu Y. Chia [31], Francesco Chiadini [102,74], Roberto Chierici [103], Andrea Chincarini [63], Antonino Chiummo [30], Gihyuk Cho [104], Heesuk S. Cho [105], Min-a Cho [83], Nelson Christensen [71], Qi Chu [72], Sheon Chua [78], Ka-wai W. Chung [101], Shinkee Chung [72], Giacomo Ciani [58,59], Pawel Ciecielag [61], Marek Cieślar [61], Alexei A. Ciobanu [62], Riccardo Ciolfi [106,59], Francesco Cipriano [71], Alessio Cirone [88,63], Filiberto Clara [48], James A. Clark [84], Patrick Clearwater [107], Sebastien Clesse [79], Frederic Cleva [71], Eugenio Coccia [17,18], Pierre-francois Cohadon [78], David Cohen [29], Marta Colleoni [108], Christophe G. Collette [109], Christopher Collins [13], Monica Colpi [46,47], Marcio Constancio Jr. [15], Livia Conti [59], Sam J. Cooper [13], Paul Corban [7], Thomas R. Corbitt [2], Isabel Cordero-Carrión [110], Silvia Corezzi [41,42], Kenneth R. Corley [111], Neil Cornish [60], David Corre [29], Alessandra Corsi [91], Stefano Cortese [30], Cesar A. Costa [15], Roberto Cotesta [82], Michael W. Coughlin [1], Scott B. Coughlin [112,14], Jeanpierre Coulon [71], Stefan T. Countryman [111], Peter Couvares [1], Pep B. Covas [108], David M. Coward [72], Matthew J. Cowart [7], Dennis C. Coyne [1], Robert Coyne [113], Jolien D. E. Creighton [23], Teviet D. Creighton [16], Jonathan Cripe [2], Michael Croquette [78], Sgwynne G. Crowder [114], Jean-rene Cudell [44], Torrey J. Cullen [2], Alan Cumming [52], Rebecca Cummings [52], Liam Cunningham [52], Elena Cuoco [30], Malgorzata Curylo [80], Tito Dal Canton [82], Gergely Dálya [115], Aykutlu Dana [55], Lara M. Daneshgaran-Bajastani [116], Beatrice D'Angelo [88,63], Stefan L. Danilishin [9,10], Sabrina D'Antonio [33], Karsten Danzmann [10,9], Christian Darsow-Fromm [117], Arnab Dasgupta [118], Laurence E. H. Datrier [52], Vincenzo Dattilo [30], Ishant Dave [64], Michel Davier [29], Gareth S. Davies [119], Derek Davis [43], Edward J. Daw [120], Dan DeBra [55], Malathi Deenadayalan [3], Jerome Degallaix [22], Martina De Laurentis [86,5], Samuel Deléglise [78], Matthew Delfavero [67], Nicola De Lillo [52], Walter Del Pozzo [56,21], Lindsay M. DeMarchi [14], Virginia D'Emilio [112], Nicholas Demos [53], Thomas Dent [119], Roberto De Pietri [121,122], Rosario De Rosa [86,5], Camilla De Rossi [30], Riccardo DeSalvo [123], Omar de Varona [9,10], Sanjeev Dhurandhar [3], Mario C. Díaz [16], Mauricio Diaz-Ortiz Jr. [31], Tim Dietrich [38], Luciano Di Fiore [5], Chiara Di Fronzo [13], Cinzia Di Giorgio [73,74], Fabrizio Di Giovanni [94], Matteo Di Giovanni [124,125], Tristano Di Girolamo [86,5], Alberto Di Lieto [56,21], Binlei Ding [109], Sibilla Di Pace [126,34], Irene Di Palma [126,34], Francesco Di Renzo [56,21], Atul K. Divakarla [31], Artemiy Dmitriev [13], Zoheyr Doctor [100], Fred Donovan [53], Katherine L. Dooley [112], Suresh Doravari [3], Iain Dorrington [112], Thomas P. Downes [23], Marco Drago [17,18], Jenne C. Driggers [48], Zhihui Du [90], Jean-gregoire Ducoin [29], Peter Dupej [52], Ofelia Durante [73,74], Domenico D'Urso [127,128], Sheila E. Dwyer [48], Paul J. Easter [6], Graeme Eddolls [52], Bruce Edelman [77], Tega B. Edo [120], Oliver Edy [129], Anamaria Effler [7], Phil Ehrens [1], Johannes Eichholz [8], Stephen S. Eikenberry [31], Marc Eisenmann [35], Robert A. Eisenstein [53], Aldo Ejlli [112], Lucianolucianikerrico Errico [86,5], Reed C. Essick [100], Hector Estelles [108], Dimitri Estevez [35], Zachariah B. Etienne [130], Todd Etzel [1], Matthew Evans [53], Tom M. Evans [7], Rebecca E. Ewing [131], Viviana Fafone [92,33,17], Stephen Fairhurst [112], Xilong Fan [90], Stefania Farinon [63], Benjamin Farr [77], Will M. Farr [98,99], Edward J. Fauchon-Jones [112], Marc Favata [37], Maxime Fays [120], Mariana Fazio [132], Jon Feicht [1], Martin M. Fejer [55],

Fangchen Feng [27], Edit Fenyvesi [54,133], Deborah L. Ferguson [84],
Alvaro Fernandez-Galiana [53], Isidoro Ferrante [56,21], Elvis C. Ferreira [15], Tabata A. Ferreira [15],
Francesco Fidecaro [56,21], Irene Fiori [30], Donatella Fiorucci [17,18], Maya Fishbach [100],
Ryan P. Fisher [40], Rosalba Fittipaldi [134,74], Margot Fitz-Axen [45], Vincenzo Fiumara [135,74],
Raffaele Flaminio [35,136], Erik Floden [45], Eric Flynn [28], Heather Fong [89], Antonio A. Font [94,137],
Perry Forsyth [8], Jean-daniel Fournier [71], Sergio Frasca [126,34], Franco Frasconi [21],
Zsolt Frei [115], Andreas Freise [13], Raymond Frey [77], Valentin Frey [29], Peter Fritschel [53],
Valery V. Frolov [7], Gabriele Fronzè [138], Paul Fulda [31], Michael Fyffe [7], Hunter A. Gabbard [52],
Bhooshan U. Gadre [82], Sebastian M. Gaebel [13], Jonathan R. Gair [82], Shanika Galaudage [6],
Dhruva Ganapathy [53], Sharad G. Gaonkar [3], Cecilio García-Quirós [108], Fabio Garufi [86,5],
Bubba Gateley [48], Sergio Gaudio [36], Gayathri Gayathri [139], Gianluca Gemme [63],
Eric Genin [30], Alberto Gennai [21], Daniel George [20], Jogy George [64], Laszlo Gergely [140],
Sudarshan Ghonge [84], Abhirup Ghosh [82], Archisman Ghosh [141,142,143,38], Shaon Ghosh [23],
Bruno Giacomazzo [124,125], Joe A. Giaime [2,7], Dwayne D. Giardina [7], Des R. Gibson [66],
Chalisa Gier [24], Kiranjyot Gill [111], Jane Glanzer [2], Jan Gniesmer [117], Patrick Godwin [131],
Evan Goetz [2,93], Ryan Goetz [31], Niklas Gohlke [9,10], Boris Goncharov [6], Gabriela González [2],
Gopakumar Gopakumar [144], Sarah E. Gossan [1], Matthieu Gosselin [30,56,21],
Romain Gouaty [35], Benjamin Grace [8], Aniello Grado [145,5], Massimo Granata [22],
Alastair Grant [52], Slawomir Gras [53], Philippe Grassia [1], Corey Gray [48], Rachel Gray [52],
Giuseppe Greco [69,70], Anna C. Green [31], Rhys Green [112], Elizabeth M. Gretarsson [36],
Hannah L. Griggs [84], G. Grignani [41,42], Andrea Grimaldi [124,125], Stefan J. Grimm [17,18],
Hartmut Grote [112], Steffen Grunewald [82], Pierre Gruning [29], Gianluca M. Guidi [69,70],
Andre R. Guimaraes [2], Gerard Guixé [50], Hitesh K. Gulati [118], Yuefan Guo [38],
Anuradha Gupta [131], Anchal Gupta [1], Pawan Gupta [38], Eric K. Gustafson [1],
Dick Gustafson [146], Leila Haegel [108], Odysse Halim [18,17], Evan D. Hall [53],
Eleanor Z. Hamilton [112], Giles Hammond [52], Maria Haney [75], Manuela M. Hanke [9,10],
Jonathan Hanks [48], Chad Hanna [131], Mark D. Hannam [112], Otto A. Hannuksela [101],
Travis J. Hansen [36], Joe Hanson [7], Thomas Harder [71], Terra Hardwick [2], Haris Haris [19],
Jan Harms [17,18], Gregg M. Harry [147], Ian W. Harry [129], Raine K. Hasskew [7],
Carl-johan Haster [53], Karen Haughian [52], Fergus J. Hayes [52], James Healy [67],
Antoine Heidmann [78], Matthew C. Heintze [7], Joscha Heinze [9,10], Henrich Heitmann [71],
Frances Hellman [148], Patrice Hello [29], Gary Hemming [30], Martin Hendry [52], Siong S. Heng [52],
Eric Hennes [38], Jan-simon Hennig [9,10], Michele Heurs [9,10], Stefan Hild [149,52],
Tanja Hinderer [143,38,141], Sarah Y. Hoback [28,147], Sven Hochheim [9,10], Elyssa Hofgard [55],
David Hofman [22], Aaron M. Holgado [20], Nathan A. Holland [8], Kathy Holt [7],
Daniel E. Holz [100], Paul Hopkins [112], Christian Horst [23], James Hough [52], Eric J. Howell [72],
Charlie G. Hoy [112], Yiwen Huang [53], Moritz T. Hübner [6], Eliu A. Huerta [20],
Dominique Huet [29], Brennan Hughey [36], Victor Hui [35], Sascha Husa [108],
Sabina H. Huttner [52], Rachael Huxford [131], Tien Huynh-Dinh [7], Bartosz Idzkowski [80],
Alberto Iess [92,33], Henri Inchauspe [31], Craig Ingram [62], Giuseppe Intini [126,34], Jean M. Isac [78],
Max Isi [53], Bala R. Iyer [19], Thibaut Jacqmin [78], Sameer J. Jadhav [150], Shreejit P. Jadhav [3],
Alasdair L. James [112], Karan Jani [84], Nagaraj N. Janthalur [150], Piotr Jaranowski [151],
Deep Jariwala [31], Rafel Jaume [108], Alex C. Jenkins [152], Jun Jiang [31], Grace R. Johns [40],
Aaron W. Jones [13], Ian I. Jones [153], Jeff D. Jones [48], Philip Jones [13], Russell Jones [52],
Reinier J. G. Jonker [38], Ju Ju [72], Jonas Junker [9,10], Chinmay V. Kalaghatgi [112],
Vassiliki Kalogera [14], Brittany Kamai [1], Shivaraj Kandhasamy [3], Gungwon Kang [39],
Jonah B. Kanner [1], Shasvath J. Kapadia [19], Sudarshan Karki [77], Rahul Kashyap [19],
Marie Kasprzack [1], Wolfgang Kastaun [9,10], Stavros Katsanevas [30], Erik Katsavounidis [53],
William Katzman [7], Steffen Kaufer [10], Keita Kawabe [48], Fabien Kéfélian [71], David Keitel [129],
Azadeh Keivani [111], Ross Kennedy [120], Joey S. Key [154], Sudiksha Khadka [55], Farit Y. Khalili [65],
Imran Khan [17,33], Sebastian Khan [9,10], Zaki A. Khan [90], Efim A. Khazanov [155],
Nandita Khetan [17,18], Mohammad Khursheed [64], Nutsinee Kijbunchoo [8], Chunglee Kim [156],

Grace J. Kim [84], Jeongcho C. Kim [157], Kyungmin Kim [101], Won Kim [62], Whansun S. Kim [158], Young-min Kim [159], Charles Kimball [14], Peter J. King [48], Maya Kinley-Hanlon [52], Robin Kirchhoff [9,10], Jeffrey S. Kissel [48], Lisa Kleybolte [117], Sergei Klimenko [31], Tyler D. Knowles [130], Philip Koch [9,10], Sina M. Koehlenbeck [9,10], Gideon Koekoek [38,149], Soumen Koley [38], Veronica Kondrashov [1], Antonios Kontos [160], Nico Koper [9,10], Mikhail Korobko [117], William Z. Korth [1], Manoj Kovalam [72], Dan B. Kozak [1], Volker Kringel [9,10], Nv V. Krishnendu [32], Andrzej Królak [161,162], Natalie Krupinski [23], Gerrit Kuehn [9,10], Anil Kumar [150], Prayush Kumar [163], Rahul Kumar [48], Rakesh Kumar [118], Sumit Kumar [19], Ling-chi Kuo [96], Adam Kutynia [161], Benjamin D. Lackey [82], Danny Laghi [56,21], Emile Lalande [164], Lam L. Lam [101], Astrid Lamberts [71,165], Michael Landry [48], Benjamin B. Lane [53], Ryan N. Lang [166], Jacob Lange [67], Brian Lantz [55], Robert K. Lanza [53], Iuri La Rosa [35], Angelique Lartaux-Vollard [29], Paul D. Lasky [6], Michael Laxen [7], Albert Lazzarini [1], Claudia Lazzaro [59], Paola Leaci [126,34], Sean Leavey [9,10], Yannick K. Lecoeuche [48], Chang-hwan H. Lee [105], Hyung-mok M. Lee [167], Hyungwon W. Lee [157], Joongoo Lee [104], Kyung-ha Lee [55], Johannes Lehmann [9,10], Nicolas Leroy [29], Nicolas Letendre [35], Yuri Levin [6], Alvin K. Y. Li [101], Jin Li [90], Kaye li [101], Tjonnie G. F. Li [101], Xiang Li [49], Frank Linde [168,38], Seth D. Linker [116], Jethro N. Linley [52], Tyson B. Littenberg [169], Liu Liu [9,10], Xiaoshu Liu [23], Miquel Llorens-Monteagudo [94], Ka-lok Lo [1], Alexandra Lockwood [170], Lionel T. London [53], Alessandro Longo [171,172], Matteo Lorenzini [17,18], Vincent Loriette [173], Marc Lormand [7], Giovanni Losurdo [21], James D. Lough [9,10], Carlos O. Lousto [67], Geoffrey Lovelace [28], Harald Lück [10,9], Diana Lumaca [92,33], Andrew P. Lundgren [129], Ma Yiqiu [49], Ronaldas Macas [112], Sean Macfoy [24], Myron MacInnis [53], Duncan M. Macleod [112], Ian O. MacMillan [147], Adrian Macquet [71], Ignacio Magaña Hernandez [23], Fabian Magaña-Sandoval [31], Ryan M. Magee [131], Ettore Majorana [34], Ivan Maksimovic [173], Asmita Malik [64], Catherine Man [71], Vuk Mandic [45], Valentina Mangano [52,126,34], Georgia L. Mansell [48,53], Michael Manske [23], Maddalena Mantovani [30], Michela Mapelli [58,59], Fabio Marchesoni [57,42,174], Frederique Marion [35], Szabolcs Márka [111], Zsuzsanna Márka [111], Charalampos Markakis [12], Ashot S. Markosyan [55], Aaron Markowitz [1], Ed Maros [1], Antonio Marquina [110], Sylvain Marsat [27], Filippo Martelli [69,70], Ian W. Martin [52], Rodica M. Martin [37], Valerie Martinez [85], Denis V. Martynov [13], Hossein Masalehdan [117], Ken Mason [53], Elena Massera [120], Alain Masserot [35], Thomas J. Massinger [53], Mariela Masso-Reid [52], Simone Mastrogiovanni [27], Andrew Matas [82], Fabrice Matichard [1,53], Nergis Mavalvala [53], Emily Maynard [2], Joshua J. McCann [72], Richard McCarthy [48], David E. McClelland [8], Scott McCormick [7], Lee McCuller [53], Stephen C. McGuire [175], Connor McIsaac [129], Jessica McIver [1], David J. McManus [8], Terry McRae [8], Sean T. McWilliams [130], Duncan Meacher [23], Grant D. Meadors [6], Moritz Mehmet [9,10], Ajit K. Mehta [19], Elena Mejuto Villa [123,74], Andrew Melatos [107], Gregory Mendell [48], Adam A. Mercer [23], Lorenzo Mereni [22], Kara Merfeld [77], Edmond L. Merilh [48], Jonathan D. Merritt [77], Mourad Merzougui [71], Syd Meshkov [1], Chris Messenger [52], Cody Messick [176], Remi Metzdorff [78], Patrick M. Meyers [107], Fabian Meylahn [9,10], Ashish Mhaske [3], Andrea Miani [124,125], Haixing Miao [13], Ioannis Michaloliakos [31], Christophe Michel [22], Hannah Middleton [107], Leopoldo Milano [86,5], Andrewlawrence L. Miller [31,126,34], Meg Millhouse [107], Joseph C. Mills [112], Edoardo Milotti [177,26], Michael C. Milovich-Goff [116], Olivier Minazzoli [71,178], Yuri Minenkov [33], Alec Mishkin [31], Chandra Mishra [179], Timesh Mistry [120], Sanjit Mitra [3], Valery P. Mitrofanov [65], Guenakh Mitselmakher [31], Richard Mittleman [53], Geoffrey Mo [53], Kentaro Mogushi [93], Satyanarayan R. P. Mohapatra [53], Siddharth R. Mohite [23], Manel Molina-Ruiz [148], Marina Mondin [116], Matteo Montani [69,70], Christopher J. Moore [13], Dan Moraru [48], Filip Morawski [61], Gerardo Moreno [48], Soichiro Morisaki [89], Benoit Mours [180], Conor M. Mow-Lowry [13], Simone Mozzon [129], Federico Muciaccia [126,34],

Arunava Mukherjee [52], Debnandini Mukherjee [131], Soma Mukherjee [16], Subroto Mukherjee [118], Nikhil Mukund [9,10], Adam Mullavey [7], Jesper Munch [62], Erik A. Muñiz [43], Peter G. Murray [52], Alessandro Nagar [95,138,181], Ilaria Nardecchia [92,33], Luca Naticchioni [126,34], Rajesh K. Nayak [182], Benjamin F. Neil [72], Joshua Neilson [123,74], Gijs Nelemans [183,38], Timothy J. N. Nelson [7], Marina Nery [9,10], Ansel Neunzert [146], Kwan-yeung Y. Ng [53], Sebastian Ng [62], Catherine Nguyen [27], Philippe Nguyen [77], David Nichols [143,38], Shania A. Nichols [2], Samaya Nissanke [143,38], Flavio Nocera [30], Minkyun Noh [53], Chris North [112], Devon Nothard [184], Laura K. Nuttall [129], Jason Oberling [48], Brendan D. O'Brien [31], Gor Oganesyan [17,18], Greg H. Ogin [185], John J. Oh [158], Sanghoon H. Oh [158], Frank Ohme [9,10], Hiroaki Ohta [89], Marcos A. Okada [15], Miquel Oliver [108], Christian Olivetto [30], Patrick Oppermann [9,10], Richard Oram [7], Brian O'Reilly [7], Rich G. Ormiston [45], Luis F. Ortega [31], Richard O'Shaughnessy [67], Serguei Ossokine [82], Charles Osthelder [1], David J. Ottaway [62], Harry Overmier [7], Ben J. Owen [91], Alexander E. Pace [131], Giulia Pagano [56,21], Michael A. Page [72], Giulia Pagliaroli [17,18], Archana Pai [139], Siddhesh A. Pai [64], Jordan R. Palamos [77], Oleg Palashov [155], Cristiano Palomba [34], Howard Pan [96], Pratap K. Panda [150], Tsun-ho Pang [38], Chris Pankow [14], Francesco Pannarale [126,34], Brijesh C. Pant [64], Federico Paoletti [21], Andrea Paoli [30], Abhishek Parida [3], William Parker [7,175], Daniela Pascucci [52,38], Antonio Pasqualetti [30], Roberto Passaquieti [56,21], Diego Passuello [21], Barbara Patricelli [56,21], Ethan Payne [6], Brynley L. Pearlstone [52], Thida C. Pechsiri [31], Ari J. Pedersen [43], Mike Pedraza [1], Arnaud Pele [7], Steven Penn [186], Albino Perego [124,125], Carlos J. Perez [48], Perigois Périgois [35], Antonio Perreca [124,125], Stephane Perriès [103], Jan Petermann [117], Harald P. Pfeiffer [82], Margot Phelps [9,10], Khun S. Phukon [3,168,38], Ornella J. Piccinni [126,34], Mikhael Pichot [71], Marco Piendibene [56,21], Francesco Piergiovanni [69,70], Vincenzo Pierro [123,74], Gabriel Pillant [30], Laurent Pinard [22], Innocenzo M. Pinto [123,74,95], Krzysztof Piotrzkowski [79], Marc Pirello [48], Matthew Pitkin [187], Wolfango Plastino [171,172], Rosa Poggiani [56,21], Yat-tung T. Pong [101], Sarah Ponrathnam [3], Pasquale Popolizio [30], Ed K. Porter [27], Jade Powell [188], Atul K. Prajapati [118], Kiran Prasai [55], Raghurama Prasanna [150], Geraint Pratten [13], Tanner Prestegard [23], Maria Principe [123,95,74], Giovanni A. Prodi [124,125], Leonid Prokhorov [13], Michele Punturo [42], Paola Puppo [34], Michael Pürrer [82], Hong Qi [112], Volker Quetschke [16], Pedro J. Quinonez [36], Fred J. Raab [48], Geert Raaijmakers [143,38], Hugh Radkins [48], Nicholas Radulesco [71], Peter Raffai [115], Hanna Rafferty [189], Sendhil Raja [64], Rajan Rajan [64], Binod Rajbhandari [91], Malik Rakhmanov [16], Karla E. Ramirez [16], Antoni Ramos-Buades [108], Javed Rana [3], Kaushik Rao [14], Piero Rapagnani [126,34], Vivien Raymond [112], Massimiliano Razzano [56,21], Jocelyn Read [28], Tania Regimbau [35], Luca Rei [63], Stuart Reid [24], David H. Reitze [1,31], Piero Rettegno [138,190], Fulvio Ricci [126,34], Colter J. Richardson [36], Jonathan W. Richardson [1], Paul M. Ricker [20], Gunnar Riemenschneider [190,138], Keith Riles [146], Monica Rizzo [14], Norna A. Robertson [1,52], Florent Robinet [29], Alessio Rocchi [33], Ramon D. Rodriguez-Soto [36], Loic Rolland [35], Jameson G. Rollins [1], Vincent J. Roma [77], Marco Romanelli [76], Rocco Romano [4,5], Chandra L. Romel [48], Isobel M. Romero-Shaw [6], Janeen H. Romie [7], Caitlin A. Rose [23], Dakota Rose [28], Kyle Rose [184], Dorota Rosińska [80], Shawn G. Rosofsky [20], Michael P. Ross [170], Sheila Rowan [52], Samuel J. Rowlinson [13], Palash K. Roy [16], Santosh Roy [3], Soumen Roy [191], Paolo Ruggi [30], Guntis Rutins [66], Kyle Ryan [48], Surabhi Sachdev [131], Travis Sadecki [48], Mairi Sakellariadou [152], Om S. Salafia [192,46,47], Livio Salconi [30], Muhammed Saleem [32], Anuradha Samajdar [38], Eduardo J. Sanchez [1], Luis E. Sanchez [1], Nicolas Sanchis-Gual [193], Jaclyn R. Sanders [194], Kevin A. Santiago [37], Edison Santos [71], Nikhil Sarin [6], Benoit Sassolas [22], B S. Sathyaprakash [131,112], Orion Sauter [35], Richard L. Savage [48], Vaibhav Savant [3], Disha Sawant [139], Sihem Sayah [22], Dean Schaetzl [1], Paul Schale [77], Mark Scheel [49], Jacob Scheuer [14], Patricia Schmidt [13], Roman Schnabel [117], Robert M. S. Schofield [77], Axel Schönbeck [117], Emil Schreiber [9,10], Bernd W. Schulte [9,10], Bernard F. Schutz [112], Otto Schwarm [185], Eyal Schwartz [7],

Jamie Scott [52], Susan M. Scott [8], Ed Seidel [20], Danny Sellers [7], Anand S. Sengupta [191], Noah Sennett [82], Daniel Sentenac [30], Valeria Sequino [63], Alexander Sergeev [155], Yoshinta Setyawati [9,10], Daniel A. Shaddock [8], Thomas Shaffer [48], Selim S. Shahriar [14], A. Sharma [17,18], Priyanka Sharma [64], Peter Shawhan [83], Hongyu Shen [20], Minori Shikauchi [89], Rosalie Shink [164], David H. Shoemaker [53], Deirdre M. Shoemaker [84], Keerti Shukla [148], Shyamsundar ShyamSundar [64], Karelle Siellez [84], Magdalena Sieniawska [61], Daniel Sigg [48], Leo P. Singer [87], Divya Singh [131], Neha Singh [80], Ayatri Singha [52], Akshat Singhal [17,34], Alicia M. Sintes [108], Valeria Sipala [127,128], Vasileios Skliris [112], Bram J. J. Slagmolen [8], Teresa J. Slaven-Blair [72], Jiri Smetana [13], Joshua R. Smith [28], Rory J. E. Smith [6], Surendranadh Somala [195], Edwin J. Son [158], Siddharth Soni [2], Borja Sorazu [52], Viola Sordini [103], Fiodor Sorrentino [63], Tarun Souradeep [3], Eric Sowell [91], Andrew P. Spencer [52], Mario Spera [58,59], Amit K. Srivastava [118], Varun Srivastava [43], Kai Staats [14], Cosmin Stachie [71], Mark Standke [9,10], Daniele A. Steer [27], Michael Steinke [9,10], Jessica Steinlechner [117,52], Sebastian Steinlechner [117], Daniel Steinmeyer [9,10], Dane Stocks [55], David J. Stops [13], Madeline Stover [184], Ken A. Strain [52], Giulia Stratta [196,70], Amber Strunk [48], Riccardo Sturani [197], Amber L. Stuver [198], Sudhagar Sudhagar [3], Vivishek Sudhir [53], Tiffany Z. Summerscales [199], Ling Sun [1], Sunil Sunil [118], Ankan Sur [61], Jishnu Suresh [89], Patrick J. Sutton [112], Bas L. Swinkels [38], Marek J. Szczepańczyk [31], Matteo Tacca [38], Simon C. Tait [52], Colm Talbot [6], Andres J. Tanasijczuk [79], David B. Tanner [31], Duo Tao [1], Marton Tápai [140], Amauri Tapia [28], Enzo N. Tapia San Martin [38], Jay D. Tasson [200], Robert Taylor [1], Rodrigo Tenorio [108], Lukas Terkowski [117], Manasadevi P. Thirugnanasambandam [3], Michael Thomas [7], Patrick Thomas [48], Jonathan E. Thompson [112], Sivananda R. Thondapu [64], Keith A. Thorne [7], Eric Thrane [6], Calley L. Tinsman [6], Saravanan R. Saravanan [3], Shubhanshu Tiwari [75,124,125], Srishti Tiwari [144], Vaibhav Tiwari [112], Karl Toland [52], Mauro Tonelli [56,21], Zeno Tornasi [52], Alejandro Torres-Forné [82], Calum I. Torrie [1], Iara Tosta e Melo [127,128], Daniel Töyrä [8], Emily A. Trail [2], Flavio Travasso [57,42], Gary Traylor [7], Maria C. Tringali [80], Aashish Tripathee [146], Agata Trovato [27], Randy J. Trudeau [1], Ka-wa W. Tsang [38], Maggie Tse [53], Rhondale Tso [49], Leo Tsukada [89], Daichi Tsuna [89], Takuya Tsutsui [89], Margherita Turconi [71], Amit S. Ubhi [13], Koh Ueno [89], Dennis Ugolini [189], Cs S. Unnikrishnan [144], Alexander L. Urban [2], Samantha A. Usman [100], Andrei C. Utina [52], Henning Vahlbruch [10], Gabriele Vajente [1], Guillermo Valdes [2], Michele Valentini [124,125], M. Vallisneri [204,205], Niels van Bakel [38], Martin van Beuzekom [38], Jo F. J. van den Brand [81,149,38], Chris Van Den Broeck [38,201], Daniel C. Vander-Hyde [43], Laura van der Schaaf [38], Joris V. Van Heijningen [72], Marielle A. van Veggel [52], Marco Vardaro [58,59], Vijay Varma [49], Steve Vass [1], Matyas Vasúth [54], Alberto Vecchio [13], Gabriele Vedovato [59], John Veitch [52], Peter J. Veitch [62], Krishna Venkateswara [170], Gautam Venugopalan [1], Didier Verkindt [35], Doga Veske [111], Flavio Vetrano [69,70], Andrea Viceré [69,70], Aaron D. Viets [202], Serena Vinciguerra [13], David J. Vine [66], Jeanyves Vinet [71], Salvatore Vitale [53], Francisco Hernandez Vivanco [6], Thomas Vo [43], Helios Vocca [41,42], Cheryl Vorvick [48], Sergey P. Vyatchanin [65], Andrew R. Wade [8], Leslie E. Wade [184], Madeline Wade [184], Rob Walet [38], Marissa Walker [28], Gavin S. Wallace [24], Larry Wallace [1], Sinead Walsh [23], Jonathan Z. Wang [146], Sibo Wang [20], Wenhui H. Wang [16], Yifan F. Wang [101], Robert L. Ward [8], Zane A. Warden [36], Jim Warner [48], Michal Was [35], Jennifer Watchi [109], Betsy Weaver [48], Li-wei Wei [9,10], Michael Weinert [9,10], Alan J. Weinstein [1], Rainer Weiss [53], Felix Wellmann [9,10], Linqing Wen [72], Peter Weßels [9,10], Jonathan W. Westhouse [36], Karl Wette [8], John T. Whelan [67], Bernard F. Whiting [31], Chris Whittle [53], Dennis M. Wilken [9,10], Daniel Williams [52], Roy D. Williams [203], Andrew R. Williamson [129], Joshua L. Willis [1], Benno Willke [10,9], Walter Winkler [9,10], Christopher C. Wipf [1], Holger Wittel [9,10], Graham Woan [52], Janis Woehler [9,10], Jared K. Wofford [67], Chun-fung Wong [101], Jennifer L. Wright [52], David S. Wu [9,10],

Daniel M. Wysocki [67], Liting Xiao [1], Hiro Yamamoto [1], Le Yang [132], Yang Yang [31], Ziyan Yang [45], Min-jet J. Yap [8], Maher Yazback [31], David W. Yeeles [112], Hang Yu [53], Haocun Yu [53], Shingheirobin Yuen [101], Adam K. Zadrożny [16], Adam Zadrożny [161], Michele Zanolin [36], Tatiana Zelenova [30], Jean-pierre Zendri [59], Michael Zevin [14], Jue Zhang [72], Liyuan Zhang [1], Teng Zhang [52], Chunnong Zhao [72], Guoying Zhao [109], Minchuan Zhou [14], Zifan Zhou [14], Xingjiang J. Zhu [6], Aaron B. Zimmerman [176], Michael E. Zucker [53,1], John Zweizig [1], The LIGO Scientific Collaboration, The Virgo Collaboration

[1] *LIGO, California Institute of Technology, Pasadena, CA 91125, USA*
[2] *Louisiana State University, Baton Rouge, LA 70803, USA*
[3] *Inter-University Centre for Astronomy and Astrophysics, Pune 411007, India*
[4] *Dipartimento di Farmacia, Università di Salerno, I-84084 Fisciano, Salerno, Italy*
[5] *INFN, Sezione di Napoli, Complesso Universitario di Monte S.Angelo, I-80126 Napoli, Italy*
[6] *OzGrav, School of Physics & Astronomy, Monash University, Clayton 3800, Victoria, Australia*
[7] *LIGO Livingston Observatory, Livingston, LA 70754, USA*
[8] *OzGrav, Australian National University, Canberra, Australian Capital Territory 0200, Australia*
[9] *Max Planck Institute for Gravitational Physics (Albert Einstein Institute), D-30167 Hannover, Germany*
[10] *Leibniz Universität Hannover, D-30167 Hannover, Germany*
[11] *Theoretisch-Physikalisches Institut, Friedrich-Schiller-Universität Jena, D-07743 Jena, Germany*
[12] *University of Cambridge, Cambridge CB2 1TN, UK*
[13] *University of Birmingham, Birmingham B15 2TT, UK*
[14] *Center for Interdisciplinary Exploration & Research in Astrophysics (CIERA), Northwestern University, Evanston, IL 60208, USA*
[15] *Instituto Nacional de Pesquisas Espaciais, 12227-010 São José dos Campos, São Paulo, Brazil*
[16] *The University of Texas Rio Grande Valley, Brownsville, TX 78520, USA*
[17] *Gran Sasso Science Institute (GSSI), I-67100 L'Aquila, Italy*
[18] *INFN, Laboratori Nazionali del Gran Sasso, I-67100 Assergi, Italy*
[19] *International Centre for Theoretical Sciences, Tata Institute of Fundamental Research, Bengaluru 560089, India*
[20] *NCSA, University of Illinois at Urbana-Champaign, Urbana, IL 61801, USA*
[21] *INFN, Sezione di Pisa, I-56127 Pisa, Italy*
[22] *Laboratoire des Matériaux Avancés (LMA), IP2I - UMR 5822, CNRS, Université de Lyon, F-69622 Villeurbanne, France*
[23] *University of Wisconsin-Milwaukee, Milwaukee, WI 53201, USA*
[24] *SUPA, University of Strathclyde, Glasgow G1 1XQ, UK*
[25] *Dipartimento di Matematica e Informatica, Università di Udine, I-33100 Udine, Italy*
[26] *INFN, Sezione di Trieste, I-34127 Trieste, Italy*
[27] *APC, AstroParticule et Cosmologie, Université Paris Diderot, CNRS/IN2P3, CEA/Irfu, Observatoire de Paris, Sorbonne Paris Cité, F-75205 Paris Cedex 13, France*
[28] *California State University Fullerton, Fullerton, CA 92831, USA*
[29] *LAL, Univ. Paris-Sud, CNRS/IN2P3, Université Paris-Saclay, F-91898 Orsay, France*
[30] *European Gravitational Observatory (EGO), I-56021 Cascina, Pisa, Italy*
[31] *University of Florida, Gainesville, FL 32611, USA*
[32] *Chennai Mathematical Institute, Chennai 603103, India*
[33] *INFN, Sezione di Roma Tor Vergata, I-00133 Roma, Italy*
[34] *INFN, Sezione di Roma, I-00185 Roma, Italy*
[35] *Laboratoire d'Annecy de Physique des Particules (LAPP), Univ. Grenoble Alpes, Université Savoie Mont Blanc, CNRS/IN2P3, F-74941 Annecy, France*
[36] *Embry-Riddle Aeronautical University, Prescott, AZ 86301, USA*
[37] *Montclair State University, Montclair, NJ 07043, USA*
[38] *Nikhef, Science Park 105, 1098 XG Amsterdam, The Netherlands*
[39] *Korea Institute of Science and Technology Information, Daejeon 34141, South Korea*
[40] *Christopher Newport University, Newport News, VA 23606, USA*
[41] *Università di Perugia, I-06123 Perugia, Italy*
[42] *INFN, Sezione di Perugia, I-06123 Perugia, Italy*
[43] *Syracuse University, Syracuse, NY 13244, USA*
[44] *Université de Liège, B-4000 Liège, Belgium*
[45] *University of Minnesota, Minneapolis, MN 55455, USA*
[46] *Università degli Studi di Milano-Bicocca, I-20126 Milano, Italy*
[47] *INFN, Sezione di Milano-Bicocca, I-20126 Milano, Italy*
[48] *LIGO Hanford Observatory, Richland, WA 99352, USA*
[49] *Caltech CaRT, Pasadena, CA 91125, USA*
[50] *Departament de Física Quàntica i Astrofísica, Institut de Ciències del Cosmos (ICCUB), Universitat de Barcelona (IEEC-UB), E-08028 Barcelona, Spain*
[51] *Dipartimento di Medicina, Chirurgia e Odontoiatria "Scuola Medica Salernitana", Università di Salerno, I-84081 Baronissi, Salerno, Italy*
[52] *SUPA, University of Glasgow, Glasgow G12 8QQ, UK*
[53] *LIGO, Massachusetts Institute of Technology, Cambridge, MA 02139, USA*
[54] *Wigner RCP, RMKI, H-1121 Budapest, Konkoly Thege Miklós út 29-33, Hungary*
[55] *Stanford University, Stanford, CA 94305, USA*
[56] *Università di Pisa, I-56127 Pisa, Italy*
[57] *Università di Camerino, Dipartimento di Fisica, I-62032 Camerino, Italy*
[58] *Università di Padova, Dipartimento di Fisica e Astronomia, I-35131 Padova, Italy*
[59] *INFN, Sezione di Padova, I-35131 Padova, Italy*
[60] *Montana State University, Bozeman, MT 59717, USA*
[61] *Nicolaus Copernicus Astronomical Center, Polish Academy of Sciences, 00-716, Warsaw, Poland*
[62] *OzGrav, University of Adelaide, Adelaide, South Australia 5005, Australia*
[63] *INFN, Sezione di Genova, I-16146 Genova, Italy*
[64] *RRCAT, Indore, Madhya Pradesh 452013, India*
[65] *Faculty of Physics, Lomonosov Moscow State University, Moscow 119991, Russia*

[66] SUPA, University of the West of Scotland, Paisley PA1 2BE, UK
[67] Rochester Institute of Technology, Rochester, NY 14623, USA
[68] Bar-Ilan University, Ramat Gan 5290002, Israel
[69] Università degli Studi di Urbino "Carlo Bo", I-61029 Urbino, Italy
[70] INFN, Sezione di Firenze, I-50019 Sesto Fiorentino, Firenze, Italy
[71] Artemis, Université Côte d'Azur, Observatoire Côte d'Azur, CNRS, CS 34229, F-06304 Nice Cedex 4, France
[72] OzGrav, University of Western Australia, Crawley, Western Australia 6009, Australia
[73] Dipartimento di Fisica "E.R. Caianiello", Università di Salerno, I-84084 Fisciano, Salerno, Italy
[74] INFN, Sezione di Napoli, Gruppo Collegato di Salerno, Complesso Universitario di Monte S. Angelo, I-80126 Napoli, Italy
[75] Physik-Institut, University of Zurich, Winterthurerstrasse 190, 8057 Zurich, Switzerland
[76] Univ Rennes, CNRS, Institut FOTON - UMR6082, F-3500 Rennes, France
[77] University of Oregon, Eugene, OR 97403, USA
[78] Laboratoire Kastler Brossel, Sorbonne Université, CNRS, ENS-Université PSL, Collège de France, F-75005 Paris, France
[79] Université catholique de Louvain, B-1348 Louvain-la-Neuve, Belgium
[80] Astronomical Observatory Warsaw University, 00-478 Warsaw, Poland
[81] VU University Amsterdam, 1081 HV Amsterdam, The Netherlands
[82] Max Planck Institute for Gravitational Physics (Albert Einstein Institute), D-14476 Potsdam-Golm, Germany
[83] University of Maryland, College Park, MD 20742, USA
[84] School of Physics, Georgia Institute of Technology, Atlanta, GA 30332, USA
[85] Université de Lyon, Université Claude Bernard Lyon 1, CNRS, Institut Lumière Matière, F-69622 Villeurbanne, France
[86] Università di Napoli "Federico II", Complesso Universitario di Monte S.Angelo, I-80126 Napoli, Italy
[87] NASA Goddard Space Flight Center, Greenbelt, MD 20771, USA
[88] Dipartimento di Fisica, Università degli Studi di Genova, I-16146 Genova, Italy
[89] RESCEU, University of Tokyo, Tokyo, 113-0033, Japan
[90] Tsinghua University, Beijing 100084, China
[91] Texas Tech University, Lubbock, TX 79409, USA
[92] Università di Roma Tor Vergata, I-00133 Roma, Italy
[93] Missouri University of Science and Technology, Rolla, MO 65409, USA
[94] Departamento de Astronomía y Astrofísica, Universitat de València, E-46100 Burjassot, València, Spain
[95] Museo Storico della Fisica e Centro Studi e Ricerche "Enrico Fermi", I-00184 Roma, Italy
[96] National Tsing Hua University, Hsinchu City, 30013 Taiwan, People's Republic of China
[97] Charles Sturt University, Wagga Wagga, New South Wales 2678, Australia
[98] Physics and Astronomy Department, Stony Brook University, Stony Brook, NY 11794, USA
[99] Center for Computational Astrophysics, Flatiron Institute, 162 5th Ave, New York, NY 10010, USA
[100] University of Chicago, Chicago, IL 60637, USA
[101] The Chinese University of Hong Kong, Shatin, NT, Hong Kong
[102] Dipartimento di Ingegneria Industriale (DIIN), Università di Salerno, I-84084 Fisciano, Salerno, Italy
[103] Institut de Physique des 2 Infinis de Lyon (IP2I) - UMR 5822, Université de Lyon, Université Claude Bernard, CNRS, F-69622 Villeurbanne, France
[104] Seoul National University, Seoul 08826, South Korea
[105] Pusan National University, Busan 46241, South Korea
[106] INAF, Osservatorio Astronomico di Padova, I-35122 Padova, Italy
[107] OzGrav, University of Melbourne, Parkville, Victoria 3010, Australia
[108] Universitat de les Illes Balears, IAC3—IEEC, E-07122 Palma de Mallorca, Spain
[109] Université Libre de Bruxelles, Brussels 1050, Belgium
[110] Departamento de Matemáticas, Universitat de València, E-46100 Burjassot, València, Spain
[111] Columbia University, New York, NY 10027, USA
[112] Cardiff University, Cardiff CF24 3AA, UK
[113] University of Rhode Island, Kingston, RI 02881, USA
[114] Bellevue College, Bellevue, WA 98007, USA
[115] MTA-ELTE Astrophysics Research Group, Institute of Physics, Eötvös University, Budapest 1117, Hungary
[116] California State University, Los Angeles, 5151 State University Dr, Los Angeles, CA 90032, USA
[117] Universität Hamburg, D-22761 Hamburg, Germany
[118] Institute for Plasma Research, Bhat, Gandhinagar 382428, India
[119] IGFAE, Campus Sur, Universidade de Santiago de Compostela, 15782, Spain
[120] The University of Sheffield, Sheffield S10 2TN, UK
[121] Dipartimento di Scienze Matematiche, Fisiche e Informatiche, Università di Parma, I-43124 Parma, Italy
[122] INFN, Sezione di Milano Bicocca, Gruppo Collegato di Parma, I-43124 Parma, Italy
[123] Dipartimento di Ingegneria, Università del Sannio, I-82100 Benevento, Italy
[124] Università di Trento, Dipartimento di Fisica, I-38123 Povo, Trento, Italy
[125] INFN, Trento Institute for Fundamental Physics and Applications, I-38123 Povo, Trento, Italy
[126] Università di Roma "La Sapienza", I-00185 Roma, Italy
[127] Università degli Studi di Sassari, I-07100 Sassari, Italy
[128] INFN, Laboratori Nazionali del Sud, I-95125 Catania, Italy
[129] University of Portsmouth, Portsmouth, PO1 3FX, UK
[130] West Virginia University, Morgantown, WV 26506, USA
[131] The Pennsylvania State University, University Park, PA 16802, USA
[132] Colorado State University, Fort Collins, CO 80523, USA
[133] Institute for Nuclear Research (Atomki), Hungarian Academy of Sciences, Bem tér 18/c, H-4026 Debrecen, Hungary
[134] CNR-SPIN, c/o Università di Salerno, I-84084 Fisciano, Salerno, Italy
[135] Scuola di Ingegneria, Università della Basilicata, I-85100 Potenza, Italy
[136] National Astronomical Observatory of Japan, 2-21-1 Osawa, Mitaka, Tokyo 181-8588, Japan
[137] Observatori Astronòmic, Universitat de València, E-46980 Paterna, València, Spain
[138] INFN Sezione di Torino, I-10125 Torino, Italy
[139] Indian Institute of Technology Bombay, Powai, Mumbai 400 076, India
[140] University of Szeged, Dóm tér 9, Szeged 6720, Hungary
[141] Delta Institute for Theoretical Physics, Science Park 904, 1090 GL Amsterdam, The Netherlands
[142] Lorentz Institute, Leiden University, PO Box 9506, Leiden 2300 RA, The Netherlands
[143] GRAPPA, Anton Pannekoek Institute for Astronomy and Institute for High-Energy Physics, University of Amsterdam, Science Park 904, 1098 XH Amsterdam, The Netherlands

[144] Tata Institute of Fundamental Research, Mumbai 400005, India
[145] INAF, Osservatorio Astronomico di Capodimonte, I-80131 Napoli, Italy
[146] University of Michigan, Ann Arbor, MI 48109, USA
[147] American University, Washington, D.C. 20016, USA
[148] University of California, Berkeley, CA 94720, USA
[149] Maastricht University, P.O. Box 616, 6200 MD Maastricht, The Netherlands
[150] Directorate of Construction, Services & Estate Management, Mumbai 400094, India
[151] University of Białystok, 15-424 Białystok, Poland
[152] King's College London, University of London, London WC2R 2LS, UK
[153] University of Southampton, Southampton SO17 1BJ, UK
[154] University of Washington Bothell, Bothell, WA 98011, USA
[155] Institute of Applied Physics, Nizhny Novgorod, 603950, Russia
[156] Ewha Womans University, Seoul 03760, South Korea
[157] Inje University Gimhae, South Gyeongsang, 50834, South Korea
[158] National Institute for Mathematical Sciences, Daejeon 34047, South Korea
[159] Ulsan National Institute of Science and Technology, Ulsan 44919, South Korea
[160] Bard College, 30 Campus Rd, Annandale-On-Hudson, NY 12504, USA
[161] NCBJ, 05-400 Świerk-Otwock, Poland
[162] Institute of Mathematics, Polish Academy of Sciences, 00656 Warsaw, Poland
[163] Cornell University, Ithaca, NY 14850, USA
[164] Université de Montréal/Polytechnique, Montreal, Quebec H3T 1J4, Canada
[165] Lagrange, Université Côte d'Azur, Observatoire Côte d'Azur, CNRS, CS 34229, F-06304 Nice Cedex 4, France
[166] Hillsdale College, Hillsdale, MI 49242, USA
[167] Korea Astronomy and Space Science Institute, Daejeon 34055, South Korea
[168] Institute for High-Energy Physics, University of Amsterdam, Science Park 904, 1098 XH Amsterdam, The Netherlands
[169] NASA Marshall Space Flight Center, Huntsville, AL 35811, USA
[170] University of Washington, Seattle, WA 98195, USA
[171] Dipartimento di Matematica e Fisica, Università degli Studi Roma Tre, I-00146 Roma, Italy
[172] INFN, Sezione di Roma Tre, I-00146 Roma, Italy
[173] ESPCI, CNRS, F-75005 Paris, France
[174] Center for Phononics and Thermal Energy Science, School of Physics Science and Engineering, Tongji University, 200092 Shanghai, People's Republic of China
[175] Southern University and A&M College, Baton Rouge, LA 70813, USA
[176] Department of Physics, University of Texas, Austin, TX 78712, USA
[177] Dipartimento di Fisica, Università di Trieste, I-34127 Trieste, Italy
[178] Centre Scientifique de Monaco, 8 quai Antoine Ier, MC 98000, Monaco
[179] Indian Institute of Technology Madras, Chennai 600036, India
[180] Université de Strasbourg, CNRS, IPHC UMR 7178, F-67000 Strasbourg, France
[181] Institut des Hautes Etudes Scientifiques, F-91440 Bures-sur-Yvette, France
[182] IISER-Kolkata, Mohanpur, West Bengal 741252, India
[183] Department of Astrophysics/IMAPP, Radboud University Nijmegen, P.O. Box 9010, 6500 GL Nijmegen, The Netherlands
[184] Kenyon College, Gambier, OH 43022, USA
[185] Whitman College, 345 Boyer Avenue, Walla Walla, WA 99362, USA
[186] Hobart and William Smith Colleges, Geneva, NY 14456, USA
[187] Department of Physics, Lancaster University, Lancaster, LA1 4YB, UK
[188] OzGrav, Swinburne University of Technology, Hawthorn VIC 3122, Australia
[189] Trinity University, San Antonio, TX 78212, USA
[190] Dipartimento di Fisica, Università degli Studi di Torino, I-10125 Torino, Italy
[191] Indian Institute of Technology, Gandhinagar Ahmedabad Gujarat 382424, India
[192] INAF, Osservatorio Astronomico di Brera sede di Merate, I-23807 Merate, Lecco, Italy
[193] Centro de Astrofísica e Gravitação (CENTRA), Departamento de Física, Instituto Superior Técnico, Universidade de Lisboa, 1049-001 Lisboa, Portugal
[194] Marquette University, 11420 W. Clybourn St., Milwaukee, WI 53233, USA
[195] Indian Institute of Technology Hyderabad, Sangareddy, Khandi, Telangana 502285, India
[196] INAF, Osservatorio di Astrofisica e Scienza dello Spazio, I-40129 Bologna, Italy
[197] International Institute of Physics, Universidade Federal do Rio Grande do Norte, Natal RN 59078-970, Brazil
[198] Villanova University, 800 Lancaster Ave, Villanova, PA 19085, USA
[199] Andrews University, Berrien Springs, MI 49104, USA
[200] Carleton College, Northfield, MN 55057, USA
[201] Department of Physics, Utrecht University, 3584CC Utrecht, The Netherlands
[202] Concordia University Wisconsin, 2800 N Lake Shore Dr, Mequon, WI 53097, USA
[203] Institute for Astronomy, University of Edinburgh, Royal Observatory, Blackford Hill, EH9 3HJ, UK
[204] Jet Propulsion Laboratory, California Institute of Technology, 4800 Oak Grove Drive, Pasadena, CA 91109, USA
[205] Theoretical AstroPhysics Including Relativity (TAPIR), MC 350-17, California Institute of Technology, Pasadena, CA 91125, USA

ARTICLE INFO

Article history:
Received 13 March 2020
Received in revised form 17 October 2020
Accepted 5 January 2021

Keywords:
GWOSC
Scientific databases
Data representation and management

ABSTRACT

Advanced LIGO and Advanced Virgo are monitoring the sky and collecting gravitational-wave strain data with sufficient sensitivity to detect signals routinely. In this paper we describe the data recorded by these instruments during their first and second observing runs. The main data products are gravitational-wave strain time series sampled at 16384 Hz. The datasets that include this strain measurement can be freely accessed through the Gravitational Wave Open Science Center at http://gw-openscience.org, together with data-quality information essential for the analysis of LIGO and Virgo data, documentation, tutorials, and supporting software.

Code metadata

Current data version	O1 V1 and O2 R1
Permanent link to code/repository used for this data version	https://doi.org/10.7935/K57P8W9D and https://doi.org/10.7935/CA75-FM95
Legal Code License	Creative Commons Attribution International Public License 4.0
Code versioning system used	NA
Software code languages, tools, and services used	Python, Django
Compilation requirements, operating environments & dependencies	Unix, Linux, Mac, Windows
Link to documentation/manual	https://www.gw-openscience.org/O1 and https://www.gw-openscience.org/O2
Support email for questions	gwosc@igwn.org

1. Motivation and significance

Gravitational waves (GWs) are transverse waves in the space-time metric that travel at the speed of light. They are generated by accelerated masses and more precisely, to lowest order, by time changes of the mass quadrupole [1], such as in the orbital motion of a binary system of compact stars. GWs were predicted in 1916 by Albert Einstein after the final formulation of the field equations of general relativity [2,3]. They were first observed directly in 2015 [4] by the Laser Interferometer Gravitational-Wave Observatory (LIGO) [5] during its first observing run (O1), which took place from September 12, 2015 to January 19, 2016.

After an upgrade of the detectors, the second observing run (O2) took place from November 30, 2016 to August 25, 2017. Advanced Virgo [6] joined this observing run on August 1, 2017. On April 1, 2019, Advanced LIGO and Advanced Virgo initiated their third observing run (O3), lasting almost one year [7]. The analysis of O1 and O2 data produced 11 confident detections (10 binary black hole mergers [4,8–12] and 1 binary neutron star merger [13]) and 14 marginal triggers, collected and described in the Gravitational Wave Transient Catalog (GWTC-1) [14].

Notable events in this catalog are the first observed event GW150914 [4], the first three-detector event GW170814 [12] and the binary neutron star (BNS) coalescence GW170817 [13]. This latter event is the first case where gravitational and electromagnetic waves have been observed from a single source [15] offering a unique description of the physical processes at play during and after the merger of two neutron stars.

The main data product of the LIGO and Virgo detectors is a time series containing the measure of the strain, which will be described more in detail in the section 2. The LIGO Scientific Collaboration and the Virgo Collaboration (LVC) release their calibrated strain data to researchers outside the LVC and to a broader public that includes amateur scientists, students, etc. The roadmap for these data releases is described in the LIGO Data Management Plan [16] and in the Memorandum of Understanding between Virgo and LIGO [17] (Attachment A, Sec. 2.9). Two types of data release are foreseen. When GW events are discovered and published individually or in a catalog, the LVC releases short segments of GW strain data around the time of the GW events, as in the case of GWTC-1 [18]. In addition, a release of the strain recorded during the entire observation run occurs after a proprietary period of internal use, necessary also to validate and calibrate the data.

The cleaned, calibrated GW strain data related to both the O1 and O2 runs were released in January 2018 [19] and in February 2019 [20], respectively. The release of the strain data for the first block of six months of O3 is currently scheduled for April 2021, and November 2021 for the second 6-month block.

This article focuses on the already-released data from the O1 and O2 runs. Public access to these data along with extensive documentation and usage instructions are provided through the Gravitational Wave Open Science Center (GWOSC) [21] at http://gw-openscience.org. GWOSC also provides online tools for finding and viewing data, usage guidelines and tutorials. We summarize this information, and include a comprehensive bibliography describing the detectors, the data collection and calibration, the noise characterization and software packages for data analysis.

To date more than 200 scientific articles have been written using the data from the GWOSC website. These analyses confirm, complement and extend the results published by the LVC, demonstrating the impact on the scientific community of the GW data releases. The covered topics span from alternative methods to search for gravitational wave events, some leading to new detections, e.g. [22–34], to reassessed estimations of the event parameters, e.g. [35–42], studies on matter effects for the binary neutron star, e.g. [43–46], GW polarization, e.g. [47,48], black-hole ringdown, e.g. [49,50], application of machine learning techniques to GW data analysis, e.g. [51,52], search for GW lensing effects, e.g. [53,54] and many other applications to astrophysics and cosmology, e.g. [55–59]. The list of projects goes beyond published scientific research and also includes student projects, academic courses, and art installations.[1]

This paper is organized as follows. The section 2 provides insights about how the data are collected and calibrated, about data quality and simulated signal injections. The GWOSC file format and content are described in the section 3, while the section 5 gives suggestions on the tools that can be used to guide the analysis of the GW data.

2. Methods

The Advanced LIGO [5] and Advanced Virgo [6] detectors are enhanced Michelson interferometers (see a simplified description of the experimental layout in Fig. 3 of [4] and Fig. 3 of [6]). Each detector has two orthogonal arms of equal length $L_x = L_y = L$, each with two mirrors acting as test masses and forming a Fabry–Perot optical cavity. The arm length is $L = 4$ km for LIGO, and $L = 3$ km for Virgo. Advanced LIGO consists of two essentially identical detectors at Hanford, Washington and Livingston, Louisiana, while the Advanced Virgo detector is located in Cascina near Pisa, Italy.

When GWs reach Earth, they alter the detector arm lengths, stretching or contracting each one according to the wave's direction, polarization and phase. This induces a time-dependent differential arm length change $\Delta L = \delta L_x - \delta L_y = hL$, proportional to the GW strain amplitude h projected onto the detector (see e.g., [1] chap. 9, p. 470). Photodiodes continuously sense the differential length variations by measuring the interference between

[1] See http://gw-openscience.org/projects/ for the list of scientific papers and projects.

the two laser beams that return to the beam splitter from the detector arms.

While Advanced LIGO and Advanced Virgo follow a similar general scheme, each facility has a specific, though closely related, design. We refer the reader to the following references for details about the technical developments on the instrumentation and instrument controls that play a major part in reaching the sensitivities obtained during the O1 and O2 observing runs. For Advanced LIGO those include the light source (a pre-stabilized laser) [60,61], the main optics [62–69], the signal recycling mirror (used to optimize the GW signal extraction) [5,70,71], the optics suspension and seismic isolation systems [72–85], the sensing and control strategies [86–88], the automation system [89], and various techniques for the mitigation of optical contamination, stray light and thermal effects [90–93].

For Advanced Virgo [6,94] a similar list includes the high reflective coatings of the core optics [95,96], the locking, control and thermal compensation systems [97–99], and the mitigation of magnetic and seismic noises [100–103].

When the detectors are taking data in their nominal configuration, they are said to be in *observing mode* or *science mode*. This condition does not occur all the time for various technical reasons. For example, the Fabry–Perot cavities included in the detector arms have to be kept at resonance together with the power and signal recycling cavities [104]. There are periods when the control loops fail to maintain the instrument on this working point causing a non-observing period. Other possible reasons for non-observing include maintenance periods and environmental effects like earthquakes, wind and the microseismic ground motion arising from ocean storms [105,106].

The time percentage during which the detectors are in science mode is called *duty cycle* or *duty factor*. During O1 the LIGO detectors had individual duty factors of 64.6% for Hanford and 57.4% for Livingston, while in O2 it was 65.3% and 61.8%, respectively. Virgo operated with a duty factor of 85.1% during O2 (see table 1 of [7]).

If we define the *network duty factor* by the time percentage during which all the detectors in the network are in science mode simultaneously, we find 42.8% for the LIGO network during O1 and 46.1% during O2 [14]. For the LIGO–Virgo network it was 35%.

It is customary to quantify the detector sensitivity by the *range* [107,108], i.e., the distance to which sources can be observed. In Figs. 1 and 2, the *BNS range* is calculated assuming that the observed source is a coalescence of compact objects of masses of 1.4 $M_\odot$ each, the observation has a minimum threshold in signal-to-noise ratio (SNR) of 8, and the range is averaged over all possible sky locations and orientations of the source, following [107]. The figures contain also the equivalent cumulative time–volume [108] obtained by multiplying the amount of time spent observing by the observed astrophysical volume as defined by the range. The sharp drops in the *BNS range* are typically due to transient noise in the interferometer limiting its sensitivity, while the gaps are due to non-observing periods. In particular, during O2, there were two long breaks, one for end-of-year holidays and another to make improvements to the detectors. At the end of both runs there was a sensitivity drop in one of the LIGO detectors. For O1, a drop in sensitivity at LIGO Livingston was caused by electronics noise at one of the end stations while, for O2, a drop in sensitivity at LIGO Hanford was due to electrostatic charging of the test mass optics caused by an earthquake in Montana.

The plots in Figs. 1 and 2 are indicative of the performance of the individual detectors.[2] However, observations are performed jointly by Advanced LIGO and Advanced Virgo as a network. Roughly speaking, the sensitivity of the global network is determined by that of the second most sensitive detector operating at any time. Despite the lower BNS range and cumulative time–volume for Virgo, its contribution has been important for astrophysical parameter estimation, especially in determining source localization and orientation [109]. For instance, GW170814 and GW170817 were localized by the three-detector network within a few tens of square degrees while the other events were localized by the two-detector network in sky areas ranging from a few hundreds to several thousands of square degrees.

Note that the sensitive distance depends strongly on the source mass, and can be much higher (up to gigaparsecs) for higher-mass BBH systems (see e.g. Fig. 1 of Ref. [110]).

The next sections provide details on the calibration, the detector noise characterization, the data quality and signal injections.

2.1. Calibration

The differential arm length read-out of the interferometer is recorded digitally through a data acquisition system [5,6,111]. The LIGO and Virgo data acquisition systems acquire data at sampling rates $f_s = 16\,384$ Hz and 20 000 Hz, respectively. The Virgo data is digitally converted to the same sampling rate as LIGO prior to any analysis.

A calibration procedure [112–117] is applied to produce the dimensionless strain from the differential arm length read-out. For both the Advanced LIGO and Advanced Virgo detectors, the calibration procedure creates a digital time series, $h(t)$, from the detector control system channels. Details of the production and characterization of $h(t)$ can be found in [118,119]. The calibration uncertainty estimation and residual systematic errors are discussed in [119–121]. The strain time series include both detector noise and any astrophysical signal that might be present.

Multiple versions of the calibrated data are produced as more precise measurements or instrument models become available. A first strain $h(t)$ is initially produced online using calibration parameters measured just before the observing period starts. This data stream is analyzed within a few seconds to generate alerts when an event is detected thus allowing follow-up observations by other facilities [122]. Other offline versions of the calibration is produced later, offline, to include improvements to the calibration models or filters, to resolve dropouts in the initial online version or after applying noise cleaning procedures. This data stream is used in the production of the final search results, e.g., the final event catalog.

For the O1 and O2 science runs, we released the final offline version, that has the most precise uncertainties and after applying available noise cleaning procedures. The calibration versions differ for the single event data releases depending on whether they pertain to the initial publication of the event (early version) [123–129] or to the catalog GWTC-1 publication (final version) [18].

The detector strain $h(t)$ is only calibrated between 10 Hz and 5000 Hz for Advanced LIGO [118,120] and 10 Hz and 8000 Hz for Advanced Virgo [119]. Any apparent signal outside this range cannot be trusted because it is not a faithful representation of the GW strain at those frequencies. This part of the spectrum where the data are not calibrated corresponds to the regions where the measurement noise increases rapidly, thus drastically reducing the chance for observing GWs.

2.2. Detector noise characterization and data quality

The strain measurement is impacted by multiple noise sources, such as quantum sensing noise, seismic noise, suspension thermal noise, mirror coating thermal noise, and local gravity gradient

[2] These figures are produced with data calibrated using the procedure described in the next section.

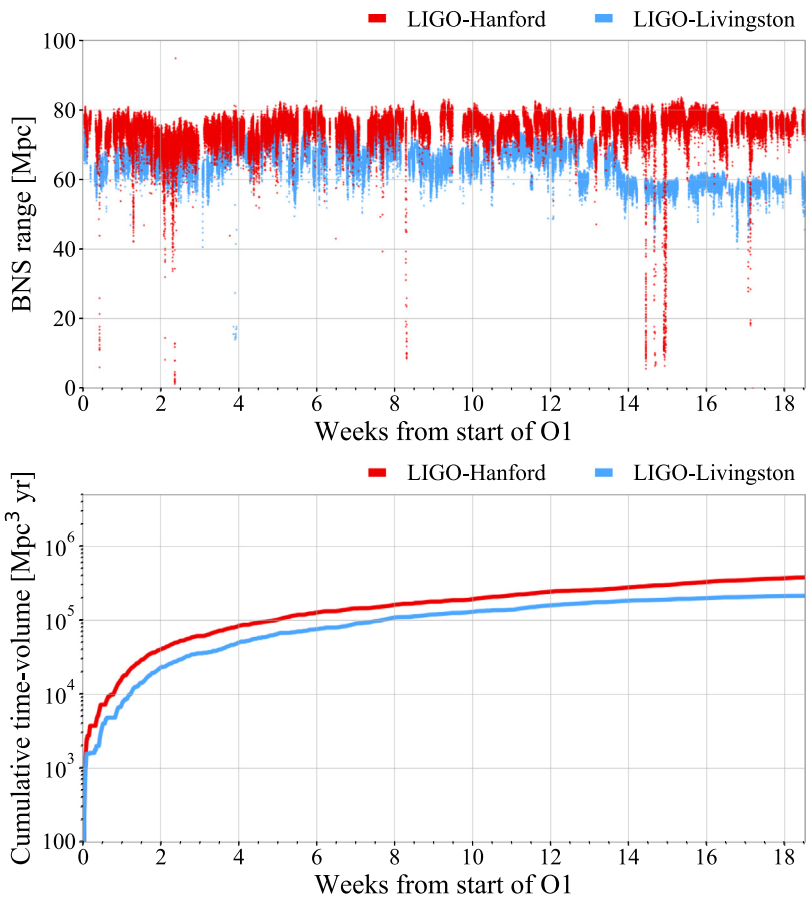

Fig. 1. Upper plot: O1 sensitivity of the Livingston and Hanford detectors to GWs as measured by the BNS range (in megaparsecs) to binary neutron-star mergers averaged over all sky positions and source orientations [107]. Lower plot: cumulative time–volume (assuming an Euclidean geometry appropriate for small redshifts) of the Livingston and Hanford detectors during O1, obtained by multiplying the observed astrophysical volume by the amount of time spent observing.

noise produced by seismic waves (called Newtonian noise) [5]. The noise budget plot for Advanced LIGO during O1 can be found in [70]. In Figs. 3 and 4 the noise budget for O2 is shown for Advanced LIGO and Advanced Virgo, respectively.

The plots show the measured noise spectrum and the contribution from various known noise sources.[3] The noise spectra indicate that the dominant noises rise steeply at high and low frequencies. This opens an observational window between tens of Hz and a few kHz. Data analysis pipelines that are used to search for gravitational-wave signals usually concentrate on frequency intervals smaller than the full calibrated bandwidth to avoid the high noise level at the extremes of this band.

The strain data are high-pass filtered at 8 Hz to avoid a number of digital signal processing problems related to spectral dynamic range and floating point precision limitation that may occur downstream when searching in the data.[4]

As shown in Figs. 3 and 4, the data contain spectral lines that can complicate searches for signals in those frequency bands [132]. These lines include calibration lines, power line harmonics, "violin" modes (resonant frequencies of mirror suspension fibers), other known instrumental lines, unknown lines and also evenly spaced combs of narrow lines, typically in exact multiples of some fundamental frequency. Further details on spectral lines during O1 and O2 can be found in [133,134] as well as on the GWOSC web pages.[5]

The detector sites are equipped with a large number of sensors that monitor both the instrumental and environmental state (see [105,106,135] for details). The measurements performed by these sensors are recorded in *auxiliary channels* that are crucial for diagnosing instrument faults or for identifying environmental perturbations. Non-Gaussian transient noise artifacts, called *glitches*, can mask or mimic true astrophysical signals [105]. Auxiliary channels provide a useful source of information for the characterization of glitches, and their mitigation. Glitches are caused by anomalous behavior in instrumental or environmental channels that couple into the GW channel. The observation of coincident glitches between the GW and auxiliary channels provides a mechanism for rejecting a detected (potential) event in the former as not astrophysical in origin. The large volume of auxiliary data (hundreds of thousands of auxiliary channels) are inspected (see [105,106,135] for details) and distilled into *data quality vetoes* that allow identification of times that are unsuitable for analysis or are likely to produce false alarms. Veto conditions are determined using systematic studies to remove glitches with high efficiency and limited loss of observation time [105]. As an example, vetoes discard glitches from electronics faults, photodiode saturations, analog-to-digital converter (ADC) and digital-to-analog converter (DAC) overflows, elevated seismic noise and computer failures. The data quality vetoes are

[3] Other useful references for the detector sensitivity are [130] for O1 and [14] for O2.

[4] See https://www.gw-openscience.org/yellow_box/ and in particular the example showing the 8 Hz roll-off at https://www.gw-openscience.org/static/images/ASDs_GW150914_1~Hz.png.

[5] http://gw-openscience.org/o1speclines and http://gw-openscience.org/o2speclines.

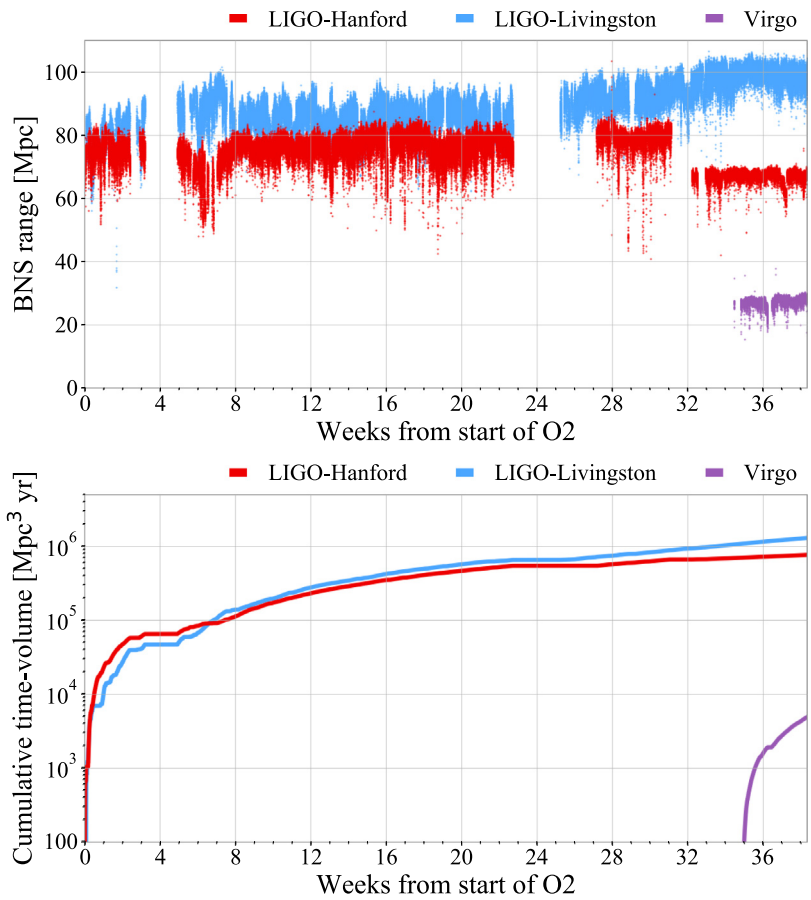

Fig. 2. Upper plot: O2 sensitivity of the Livingston, Hanford and Virgo detectors to GWs as measured by the BNS range (in megaparsecs) to binary neutron-star mergers averaged over all sky positions and source orientations [107]. Lower plot: cumulative time–volume (assuming Euclidean geometry appropriate for small redshifts) of the Livingston, Hanford and Virgo detectors during O2, obtained by multiplying the observed astrophysical volume by the amount of time spent observing. Although Virgo has a lower BNS range and cumulative time–volume, its contribution is crucial for source localization and astrophysical parameter estimation.

used by the GW searches to reduce the noise background [105] (see Sec. 3.2 for search-related usage information).

Different categories of data quality are defined according to the severity level and degree of understanding of the noise artifact. Data flagged as invalid due to severe detector malfunctioning, calibration error, or data acquisition problems, as described in [136] are typically not used for data analysis and are replaced by `NaN`s in the GWOSC data releases. We elaborate further on the various data quality categories and their usage in the section 3.[6]

Auxiliary channels are also used to subtract post-facto some well identified instrumental noise from the GW strain data. A procedure based on a linear coupling model [137] computes the transfer function that couples the witness channels to $h(t)$ and subtracts the contributing noise from the strain amplitude. This procedure was used during the second observing run in Advanced LIGO data. It achieved an increase of up to 30% of the detector sensitive volume to GWs for a broad range of compact binary systems and was most significant for the LIGO-Hanford detector [138]. In some cases data are available both before and after noise subtraction is applied (for example in the case of GW170817 [129]).

2.3. Signal injections

In addition to data quality, some metadata provide information about *hardware injections* [139] inserted into the detector data for testing and calibration. The detectors' test masses (interferometer mirrors) are physically displaced by an actuator in order to simulate the effects of a GW.[7] A simulated GW signal is introduced into the detector control system yielding a response which mimics that of a true GW. The analysis of a data segment that includes an injection allows an end-to-end test of the ability for the analysis procedure to detect and characterize the GW strain signal.

Hardware injections are also used for detector characterization to check that the auxiliary channels used for vetoes do not respond to gravitational-wave-like signals. This is a *safety* check since a channel that has no sensitivity to GWs is considered safe for use when constructing a veto. It is clearly important to keep a record of injections to avoid any confusion with real events. In the section 3 we describe how this bookkeeping is done.[8]

3. Data records

GW open data are distributed under the Creative Commons Attribution International Public License 4.0[9] through the GWOSC web pages.[10] The files can be directly downloaded one by one from this web page. However, to download large amounts of

6 See also http://gw-openscience.org/o1_details and http://gw-openscience.org/o2_details.

7 Calibration lines mentioned earlier are generated using the same process.

8 See the GWOSC web page http://gw-openscience.org/o1_inj and http://gw-openscience.org/o2_inj.

9 https://creativecommons.org/licenses/by/4.0/legalcode

10 http://gw-openscience.org/data/

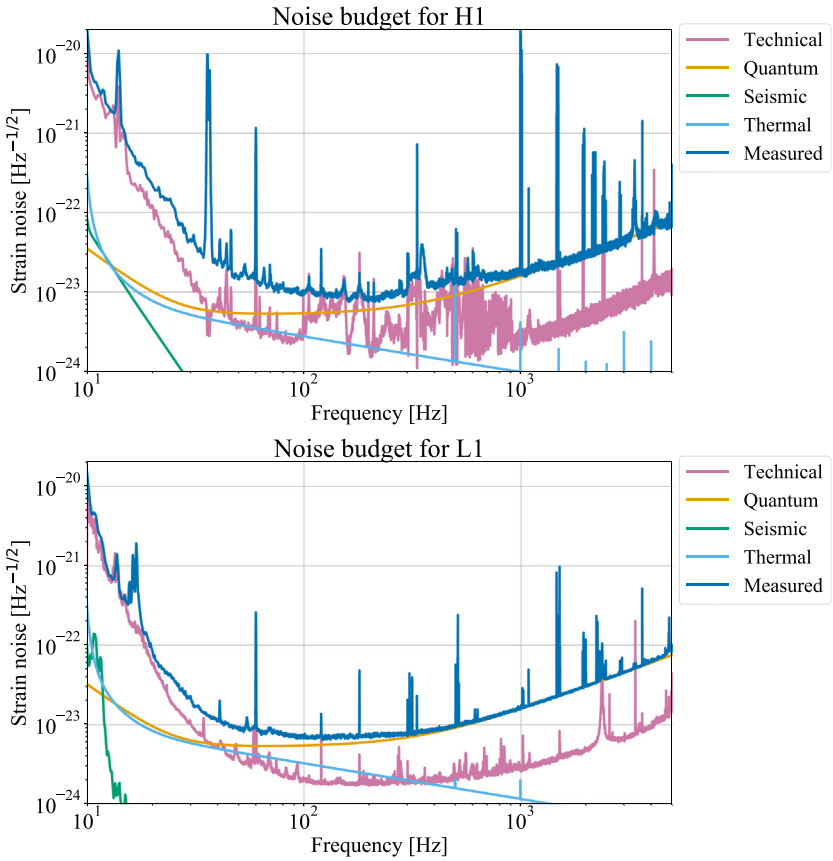

Fig. 3. Sensitivities of the Advanced LIGO detectors during the second observation run (O2), expressed as the equivalent strain noise spectrum of each detector (the blue "Measured" curves). Also shown are the known contributors to the detector noise, which sum to the measured spectrum across much, but not all of the frequency band (i.e. the measured noise spectrum is not fully explained by all known sources of noise). The quantum noise includes both shot noise (dominant at higher frequencies) and radiation pressure noise (dominant at lower frequencies). Thermal noise includes contributions from the suspensions, the substrate and coatings of the test masses. Seismic noise is computed as the ground displacement attenuated through the seismic isolation system and the suspensions chain. The seismic curves differ for H1 and L1 as actual seismic data were used for L1 while the H1 curve is a model that also includes Newtonian noise. Technical noise includes angular and length sensing/control noise for degrees of freedom that are not related to the differential arm length measurement, and other sub-dominant noises such as laser frequency, intensity and beam jitter noise, sensor and actuation noise, and Rayleigh scattering by the residual gas. The strong line features are due to the violin modes of the suspension wires, other resonance modes of the suspensions, the AC power line and its harmonics, and the calibration lines. Examples of similar plots for other data taking runs can be found in [70,131]. These noise spectra do not include any of the post-data collection noise subtraction mentioned in the text. (For interpretation of the references to color in this figure legend, the reader is referred to the web version of this article.)

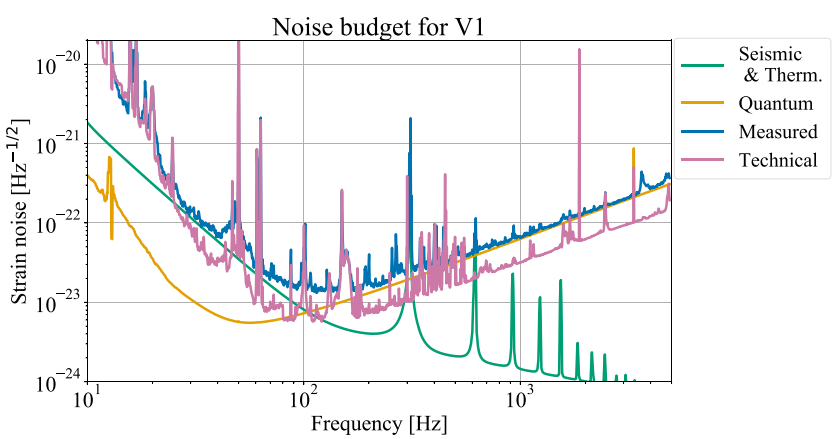

Fig. 4. Sensitivity of the Advanced Virgo detector during the O2 observation run. The meaning of the noise source contributions is the same as in Fig. 3, except for the seismic and thermal noises that are combined in this case and for the Newtonian noise which is not included. These noise spectra do not include any of the post-data collection noise subtraction mentioned in the text.

data (such as an entire observing run) the use of the distributed filesystem `CernVM-FS` [140,141] is preferred.[11] Once installed,

[11] For installation instructions, see http://gw-openscience.org/cvmfs/

Table 1
The channel names and frame types listed in this table are unique identifiers in the LIGO and Virgo data archives that allow tracing the provenance of the strain data released on GWOSC. The attribute `CLEAN` in H1 and L1 for O2 indicates that the noise subtraction procedure mentioned previously and described in [137] was used. The attributes `C02`, `DCS`, `DCH` and `Repro2A` refer to the calibration version.

Run	Det.	Channel name	Frame type
O1	H1	H1:DCS-CALIB_STRAIN_C02	H1_HOFT_C02
O1	L1	L1:DCS-CALIB_STRAIN_C02	L1_HOFT_C02
O2	H1	H1:DCH-CLEAN_STRAIN_C02	H1_CLEANED_HOFT_C02
O2	L1	L1:DCH-CLEAN_STRAIN_C02	L1_CLEANED_HOFT_C02
O2	V1	V1:Hrec_hoft_V1O2Repro2A_16384 Hz	V1O2Repro2A

this filesystem allows access to GWOSC data as files in a directory tree mounted locally on the user's computer.

The calibrated strain data of O1 [19] and O2 [20] described in this paper are conveniently divided into files of 4096 s. Short segments of 32 s and 4096 s duration for each GW event are also released.[12] The description of the data records that follows is valid both for single event release and for bulk data release.

The strain data are repackaged and resampled by GWOSC to make it more accessible to users both within the LVC and outside. Along with the native 16 384 Hz sampling rate, the data on GWOSC are also made available at 4096 Hz.[13] The downsampling is performed using the standard decimation technique implemented in `scipy.signal.decimate`[14] from the Python package `scipy` [143]. From the Nyquist–Shannon sampling theorem [144–146], the largest accessible frequency is the Nyquist frequency equal to half of the sampling rate f_s. This should be kept in mind when choosing the sampling rate to download from GWOSC, and in general when analyzing these files; in particular, because of the anti-aliasing filter's roll-off, the data sampled at 4 kHz are valid only up to frequencies of about 1700 Hz.

The publicly released data are generated from data streams in the LIGO and Virgo data archives uniquely identified by a channel name and a frame type (an internal label that specifies the content of the files). For completeness, we give the provenance of the GWOSC data in Table 1 and list the channel names and frame types used to generate the O1 and O2 dataset discussed in this article. In this table and in the following, H1 and L1 indicate the two LIGO detectors (Hanford and Livingston respectively) while V1 refers to Virgo. Downsampling (for the 4 kHz dataset) and replacement with `NaN`s of bad quality or absent data are the only modifications of the original data.

3.1. Gwosc file formats

The GW open data are delivered in two different file formats: `hdf` and `gwf`. The Hierarchical Data Format `hdf` [147] is a portable data format readable by many programming languages. The Frame format `gwf` [148] is used internally by the GW community. In addition, the data associated with GW events are also released as plain text files containing two columns with the GPS time and the corresponding strain values.

There are some differences in the structure of the file names between O1 and O2 due to the evolution of GWOSC itself. For O1 the name of the files has the structure: *obs-ifo*_LOSC_*s*_V*n*-*GPSstart-duration.extension*, where *obs* is the observatory, i.e. the site, so can have values L or H; *ifo* is the interferometer and can have values H1 or L1; `LOSC` is the previous name of GWOSC, (the L in LOSC stands for LIGO); *s* is the sampling rate in kHz with possible values 4 or 16; *n* is the version number of the file (until now we have only one version, so only V1); *GPSstart* is the starting time in GPS of the data contained in the file; *duration* is the duration in seconds of this segment of data, which value is always 4096 in this case; the *extension* can be gwf or hdf. The file names in O2 are instead of the type *obs-ifo*_GWOSC_*ObservationRun*_*s*KHZ_R*n*-*GPSstart-duration.extension*, with the same meaning of the italic letters, but in this case *obs* and *ifo* can have also the values V and V1, respectively, for Virgo data and we added the run name in the file names, so in this case *ObservationRun* is O2.

Table 2
Channel names of the GWOSC frame (`gwf`) files. In the name, *ifo* is a place holder for the interferometer name, i.e. H1, L1 or V1, and *s* the sampling rate in kHz. The `R1` substring represents the revision number of the channel name so it will become `R2` in case there is a second (revised) release, and so on.

	O1 (4 kHz sampling)	O1 (16 kHz sampling) and O2
Strain	*ifo*:LOSC-STRAIN	*ifo*:GWOSC-*s*KHZ_R1_STRAIN
Data quality mask	*ifo*:LOSC-DQMASK	*ifo*:GWOSC-*s*KHZ_R1_DQMASK
Injections mask	*ifo*:LOSC-INJMASK	*ifo*:GWOSC-*s*KHZ_R1_INJMASK

The folders (or groups) included in the `hdf` files are:

- *meta*: metadata of the file containing the following fields:
  - *Description*, e.g. "Strain data time series from LIGO",
  - *DescriptionURL*: URL of the GWOSC website,
  - *Detector*, e.g. L1, and *Observatory*, e.g. L,[15]
  - *Duration*, *GPSstart*, *UTCstart*: duration and starting time (in GPS and UTC, respectively) of the segment of data contained in the file.

  In the O2 files it was decided to add also the *StrainChannel* and *FrameType* of the original files internally used by the LVC (i.e. the content of Table 1).
- *strain*: array of $h(t)$, sampled at 4 or 16 kHz depending on the file. For the times when the detector is not in science mode or the data does not meet the minimum required data quality conditions (see next section), the strain values are set to `NaN`s. The strain $h(t)$ is a function of time, so it is accompanied by the attributes *Xstart* and *Xspacing* defining the starting GPS time of the data contained in the array and the corresponding distance in time between the points of the array.
- *quality*: this folder contains two sub-folders, one for data quality and the other for injections, each including a bitmask to indicate at each second the status of the data quality or the injections and the description of each bit of the mask, i.e. the content of Tables 3 and 4 (see section 3.2 for details).

The `gwf` files have a similar content but with a different structure. They contain 3 channels, one for the strain data, one for the data quality and one for the injections. The channel names differ slightly in O1 and O2 as described in Table 2. Note that the original files produced internally, whose channel names are listed in Table 1, contain only the strain channel, while the GWOSC files include also the data quality and injection information in the same file.

[12] http://gw-openscience.org/eventapi/

[13] In the rest of the paper the sampling rates will be indicated in kHz and rounded to the closest integer, i.e. 4 and 16 kHz means 4096 and 16 384 Hz, respectively

[14] This method applies an anti-aliasing filter based on an order-8 Chebyshev type I infinite impulse response (IIR) filter [142] before decimation.

[15] The observatory refer to the site and it is indicated by one letter, like L for Livingston. The addition of a number after the letter to indicate the detector, e.g. L1, could be useful if multiple detectors are installed in the same site, as it was at the beginning of LIGO.

3.2. Data quality and injections in gwosc files

Several types of searches are performed on the LIGO and Virgo data. Those searches are divided into four families named after the type of signals they target: Compact binary coalescences (CBC), GW bursts (BURST), continuous waves (CW) and stochastic backgrounds (STOCH).

CBC analyses (see e.g., [8,14,110,149–153]) seek signals from merging neutron stars and black holes by filtering the data with waveform templates. BURST analyses (see e.g., [154–158]) search for generic GW transients with minimal assumption on the source or signal morphology by identifying excess power in the time–frequency representation of the GW strain data. CW searches (see e.g., [159–162]) look for long-duration, continuous, periodic GW signals from asymmetries of rapidly spinning neutron stars. STOCH searches (see e.g., [163,164]) target the stochastic GW background signal which is formed by the superposition of a wide variety of independent and unresolved sources from different stages of the evolution of the Universe.

Due to the fundamental differences among these searches, some types of noise are problematic only for one or two types of search. For this reason, the data quality related to transient noises depends on the search type. It is provided inside the GWOSC files for the two GW transient searches CBC and BURST, that are most sensitive to this type of noise. The data quality information most relevant for CW and STOCH searches is in the frequency domain and it is provided as lists of instrumental lines in separate files [165–169].

Data quality and signal injection information for a given GPS second is indicated by bitmasks with a 1-Hz sampling rate. The bit meanings are given in Tables 3 and 4 for the data quality and injections, respectively. To describe data quality, different *categories* are defined. For each category, the corresponding bit in the bitmask shown in Table 3 has value 1 (good data) if in that second of time the requirements of the category are fulfilled, otherwise 0 (bad data).

The meaning of each category is the following:

DATA Failing this level indicates that LIGO and Virgo data are not available in GWOSC data because the instruments were not operating in nominal conditions. For O1 and O2, this is equivalent to failing Category 1 criteria, defined below. For these seconds of bad or absent data, NaNs have been inserted.

CAT1 (Category 1) Failing a data quality check at this category indicates a critical issue with a key detector component not operating in its nominal configuration. Since these times indicate a major known problem they are identical for each data analysis group. However, while CBC_CAT1 and BURST_CAT1 flag the same data, they exist separately in the dataset. GWOSC data during times that fail CAT1 criteria are replaced by NaN values in the strain time series. The time lost due to these critical quality issues (*dead time*) is: 1.683% (H1) and 1.039% (L1) of the run during O1; and 0.001% (H1), 0.003% (L1) and 0.053% (V1) of the run during O2 (all the percentages have been calculated with respect to the periods of science mode).

CAT2 (Category 2) Failing a data quality check at this category indicates times when there is a known, understood physical coupling between a sensor/auxiliary channel that monitors excess noise, and the strain channel [170]. The dead times corresponding to this veto for the CBC analysis are: 0.890% (H1) and 0.007% (L1) of the run during O1; 0.157% (H1) and 0.090% (L1) of the run during O2. The dead times corresponding to this veto for the BURST analysis are: 0.624% (H1) and 0.021% (L1) of the run during O1; 0.212% (H1) and 0.151% (L1) of the run during O2. CAT2 was not used for Virgo in O2.

CAT3 (Category 3) Failing a data quality check at this category indicates times when there is statistical coupling between a sensor/auxiliary channel and the strain channel which is not fully understood. This category was not used in O1 and O2 LVC searches, but it is still in the file format for historical reasons.

Table 3
Data quality bitmasks description. Data that are *not* present are replaced by NaN values in the strain time series. CBC_CAT1 and BURST_CAT1 are equivalent (see the definition of CAT1 in the text).

Bit	Short name	Description
0	DATA	Data present
1	CBC_CAT1	Pass CAT1 test
2	CBC_CAT2	Pass CAT1 and CAT2 test for CBC searches
3	CBC_CAT3	Pass CAT1 and CAT2 and CAT3 test for CBC searches
4	BURST_CAT1	Pass CAT1 test
5	BURST_CAT2	Pass CAT1 and CAT2 test for BURST searches
6	BURST_CAT3	Pass CAT1 and CAT2 and CAT3 test for BURST searches

Table 4
Meaning of the injection bits.

Bit	Short name	Description
0	NO_CBC_HW_INJ	No CBC injections
1	NO_BURST_HW_INJ	No burst injections
2	NO_DETCHAR_HW_INJ	No detector characterization injections
3	NO_CW_HW_INJ	No continuous wave injections
4	NO_STOCH_HW_INJ	No stochastic injections

As an example, [170] gives the list of all sensors/auxiliary channels used to define the CAT1 and CAT2 flags for BURST and CBC around the event GW150914.

Data quality categories are cascading: a time which fails a given category automatically fails all higher categories. Since CAT3 is not used in this specific case and only data passing CAT1 are provided, there is only the possibility that the data pass or not CAT2. However, the different analysis groups qualify the data independently: failing BURST_CAT2 does not necessarily imply failing CBC_CAT2.

The injection bitmask marks the injection-free times. Five different types of injections are usually performed: injections simulating signals searched for by CBC, BURST, CW and STOCH LVC pipelines, and injections used for detector characterization, labeled DETCHAR. For each injection type, the bit of the bitmask, whose meaning is described in Table 4, has value 1 if the injection is not present, otherwise 0.

Virgo did not perform hardware injections during O2, therefore all the bits of the injection bitmask have value 1.

4. Technical validation

The data repackaged for public use are validated by another independent internal team. In particular, this review team checks that:

- the strain vectors in the GWOSC hdf and gwf files are identical to machine precision to the corresponding strain vectors of the LVC main archives;
- the data quality and injection information given to the user correspond to what is included in the original LVC data quality database. The user can get this information in two ways: the bitmask included in the GWOSC files and the *Timeline* tool described in detail in the section 5. The output of both methods is checked against the database;

- the documentation web pages and the content of the present article contain correct and comprehensive information.

The data files, the *Timeline* and the web pages are released to the public once all those checks have been passed.

5. Usage notes

GW detectors are complex instruments, and their data reflect this complexity. For this reason, caution should be taken when searching for GW signals in the detector strain data, taking into account all the details about the usable frequency range, noise artifacts, data quality and injections discussed in this paper and in the references. In particular, the application of all data quality flags described in the previous section does *not* imply that the remaining data are free of transient noise artifacts. The user can find guidance to analyze the GW data in the tutorials and tools collected in the GWOSC website and discussed in the next subsections. The data analysis techniques used to detect GW signals and infer the source properties are described in [132] where good practices and advices to avoid common errors are also provided. The GWOSC website also contains basic information about the geographical position[16] and the current status[17] of the detectors.

5.1. Timeline

The LIGO and Virgo detectors are not always in observing mode and, even when they are, it is possible that data quality does not meet the requirements of a given analysis. For these reasons it is necessary to restrict analysis to valid *segments* of data characterized by data quality information that indicates the data is acceptable for the desired analysis. *Timeline*[18] is a tool to provide a visual representation of available valid data segments over a time interval, together with the related information about data quality and presence of injected signals (see Fig. 5 for an example with the O2 dataset). If the requested interval is short enough, this is shown at the time scale of seconds. For longer intervals, *Timeline* shows the average value of the selected data-quality bit over nonoverlapping 2^n-second subintervals.

Besides the visual representation, this tool allows the user to download the list of start and stop of the segments for a specific data quality category or injection type, and also the corresponding data.

5.2. Courses, software packages and tutorials for gw data analysis

On-line courses that provide an introduction to GW data analysis ranging from the basics to more advanced topics with hands-on exercises are available from the GWOSC website.[19] Those courses have been recorded during the GW Open Data Workshops. They include lectures on various aspects of GW science and are supported by many tutorials that can be used to understand how to read and analyze the data. The tutorials on the GOWSC website[20] are in the form of `Jupyter` notebooks [171]. They explain how to access the data, produce time–frequency spectrograms, carry out matched-filtering searches, infer astrophysical parameters, and manipulate GW localization information. A few tutorials start from first principles and use generic and broadly used analysis software such as `scipy` [143], but most are based on the specialized software packages and libraries that the LVC developed to produce observational results and other scientific products.

A list of those packages is available on the GWOSC website[21] and includes:

- the light-weight application `readligo` to access data;
- general purpose application software, such as the LSC Algorithm Library Suite (`LALSuite`) [172] and the Python package `gwpy` [173];
- search-oriented software such as `pycbc` [149,150], `GstLAL` [174] and Coherent Waveburst (`cWB`) [154];
- post-processing software for e.g., parameter estimation such as `bilby` [175], `LALInference` [176] and Bayeswave [177, 178].

All these packages are open source and freely distributed.

5.3. Summary and additional information

The LVC is committed to providing strain data from the LIGO and Virgo detectors to the public, according to the schedule outlined in the LIGO Data Management Plan [16], via the Gravitational Wave Open Science Center (GWOSC) [179]. They are also committed to providing a broad range of data analysis products to facilitate reproducing the results presented in their observational papers. Many of these data products are available through the LIGO Document Control Center (DCC); for example, data products associated with the GWTC-1 event catalog [14] can be found in [18] and [180]. Many more data offerings are planned for the future. This includes the catalog of observed events and the bulk strain data from the LIGO/Virgo O3 run. More GWOSC Open Data Workshops are also planned.

All users of these data are welcome to sign up with the GWOSC User's Group at https://www.gw-openscience.org/join/. Anyone who uses these data in publications and other public data products are requested to acknowledge GWOSC by following the guidance in [181]. Publications that acknowledge GWOSC will be listed in https://www.gw-openscience.org/projects/; email `gwosc@igwn.org` to make sure your publication(s) are included.

The Collaborations, and the GWOSC team, welcome comments and suggestions for improving these data releases and products, and their presentation on the GWOSC website [179], via email to `gwosc@igwn.org`. Questions about the use of these data products may also be sent to that email, and will be entered into our help ticket system. More general questions about LIGO, Virgo, and GW science should go to `questions@ligo.org`.

Declaration of competing interest

The authors declare that they have no known competing financial interests or personal relationships that could have appeared to influence the work reported in this paper.

Acknowledgments

This research has made use of data, software and/or web tools obtained from the Gravitational Wave Open Science Center (https://www.gw-openscience.org/), a service of LIGO Laboratory, the LIGO Scientific Collaboration and the Virgo Collaboration. LIGO Laboratory and Advanced LIGO are funded by the United States National Science Foundation (NSF) as well as the Science and Technology Facilities Council (STFC) of the United Kingdom, the Max-Planck-Society (MPS), and the State of Niedersachsen/Germany for support of the construction of Advanced

16 http://gw-openscience.org/static/param/position.txt
17 http://gw-openscience.org/detector_status/
18 http://gw-openscience.org/timeline/
19 http://gw-openscience.org/workshops/
20 http://gw-openscience.org/tutorials/
21 http://gw-openscience.org/software/

Fig. 5. The GWOSC offers immediate access to duty cycle information for data quality and injection bits through the *Timeline* (http://gw-openscience.org/timeline/). By default, the time resolution is chosen to display the entire dataset. From there, one can zoom in to smaller timescales by clicking on the display.

LIGO and construction and operation of the GEO600 detector. Additional support for Advanced LIGO was provided by the Australian Research Council. Virgo is funded, through the European Gravitational Observatory (EGO), by the French Centre National de Recherche Scientifique (CNRS), the Italian Istituto Nazionale di Fisica Nucleare (INFN) and the Dutch Nikhef, with contributions by institutions from Belgium, Germany, Greece, Hungary, Ireland, Japan, Monaco, Poland, Portugal, Spain.

The authors gratefully acknowledge the support of the United States National Science Foundation (NSF) for the construction and operation of the LIGO Laboratory and Advanced LIGO as well as the Science and Technology Facilities Council (STFC) of the United Kingdom, the Max-Planck-Society (MPS), and the State of Niedersachsen/Germany for support of the construction of Advanced LIGO and construction and operation of the GEO600 detector. Additional support for Advanced LIGO was provided by the Australian Research Council. The authors gratefully acknowledge the Italian Istituto Nazionale di Fisica Nucleare (INFN), the French Centre National de la Recherche Scientifique (CNRS) and the Foundation for Fundamental Research on Matter supported by the Netherlands Organisation for Scientific Research, for the construction and operation of the Virgo detector and the creation and support of the EGO consortium. The authors also gratefully acknowledge research support from these agencies as well as by the Council of Scientific and Industrial Research of India, the Department of Science and Technology, India, the Science & Engineering Research Board (SERB), India, the Ministry of Human Resource Development, India, the Spanish Agencia Estatal de Investigación, the Vicepresidència i Conselleria d'Innovació, Recerca i Turisme and the Conselleria d'Educació i Universitat del Govern de les Illes Balears, the Conselleria d'Educació, Investigació, Cultura i Esport de la Generalitat Valenciana, the National Science Centre of Poland, the Swiss National Science Foundation (SNSF), the Russian Foundation for Basic Research, the Russian Science Foundation, the European Commission, the European Regional Development Funds (ERDF), the Royal Society, the Scottish Funding Council, the Scottish Universities Physics Alliance, the Hungarian Scientific Research Fund (OTKA), the Lyon Institute of Origins (LIO), the Paris Île-de-France Region, the National Research, Development and Innovation Office Hungary (NKFIH), the National Research Foundation of Korea, Industry Canada and the Province of Ontario through the Ministry of Economic Development and Innovation, the Natural Science and Engineering Research Council Canada, the Canadian Institute for Advanced Research, the Brazilian Ministry of Science, Technology, Innovations, and Communications, the International Center for Theoretical Physics South American Institute for Fundamental Research (ICTP-SAIFR), the Research Grants Council of Hong Kong, the National Natural Science Foundation of China (NSFC), the Leverhulme Trust, the Research Corporation, the Ministry of Science and Technology (MOST), Taiwan and the Kavli Foundation. The authors gratefully acknowledge the support of the NSF, STFC, INFN and CNRS for provision of computational resources.

References

[1] Maggiore M. Gravitational waves, volume 1: theory and experiments. Oxford University Press; 2008.
[2] Einstein A. Approximative integration of the field equations of gravitation. Sitzungsber Preuss Akad Wiss Berlin (Math Phys) 1916;1916:688–96.
[3] Einstein A. Über Gravitationswellen. Sitzungsber Preuss Akad Wiss Berlin (Math Phys) 1918;1918:154–67.
[4] Abbott BP, et al., LIGO Scientific Collaboration, Virgo Collaboration. Observation of gravitational waves from a binary black hole merger. Phys Rev Lett 2016;116:061102.
[5] Aasi J, et al., LIGO Scientific Collaboration. Advanced LIGO. Classical Quantum Gravity 2015;32:074001.
[6] Acernese F, et al., Virgo Collaboration. Advanced Virgo: a second-generation interferometric gravitational wave detector. Classical Quantum Gravity 2015;32:024001.
[7] KAGRA Collaboration, LIGO Scientific Collaboration, and Virgo Collaboration. Prospects for observing and localizing gravitational-wave transients with Advanced LIGO, Advanced Virgo and KAGRA. 2019, Preprint at https://arxiv.org/abs/1304.0670.
[8] Abbott BP, et al., LIGO Scientific Collaboration, Virgo Collaboration. GW150914: First results from the search for binary black hole coalescence with Advanced LIGO. Phys Rev D 2016;93:122003.
[9] Abbott BP, et al., LIGO Scientific Collaboration, Virgo Collaboration. GW151226: Observation of gravitational waves from a 22-solar-mass binary black hole coalescence. Phys Rev Lett 2016;116:241103.
[10] Abbott BP, et al., LIGO Scientific Collaboration, Virgo Collaboration. Binary black hole mergers in the first Advanced LIGO observing run. Phys Rev X 2016;6:041015.
[11] Abbott BP, et al., LIGO Scientific Collaboration, Virgo Collaboration. GW170104: Observation of a 50-solar-mass binary black hole coalescence at Redshift 0.2. Phys Rev Lett 2017;118:221101.
[12] Abbott BP, et al., LIGO Scientific Collaboration, Virgo Collaboration. GW170814: A three-detector observation of gravitational waves from a binary black hole coalescence. Phys Rev Lett 2017;119:141101.

[13] Abbott BP, et al., LIGO Scientific Collaboration, Virgo Collaboration. GW170817: Observation of gravitational waves from a binary neutron star inspiral. Phys Rev Lett 2017;119:161101.
[14] Abbott BP, et al., LIGO Scientific Collaboration, Virgo Collaboration. GWTC-1: A gravitational-wave transient catalog of compact binary mergers observed by LIGO and virgo during the first and second observing runs. Phys Rev X 2019;9:031040, arXiv:1811.12907.
[15] Abbott BP, et al. Multi-messenger observations of a binary neutron star merger. Astrophys J 2017;848:L12.
[16] Anderson S, Williams R. LIGO data management plan. 2017, URL https://dcc.ligo.org/LIGO-M1000066/public.
[17] LIGO Scientific Collaboration and Virgo Collaboration. Memorandum of understanding between Virgo and LIGO. LIGO-M060038, VIR-0091A, 2019, https://dcc.ligo.org/LIGO-M060038/public.
[18] LIGO Scientific Collaboration and Virgo Collaboration. LIGO/Virgo GWTC-1 data release. 2018, URL https://www.gw-openscience.org/GWTC-1/.
[19] LIGO Scientific Collaboration and Virgo Collaboration. LIGO/Virgo O1 data release. 2018, URL https://www.gw-openscience.org/O1/.
[20] LIGO Scientific Collaboration and Virgo Collaboration. LIGO/Virgo O2 data release. 2019, URL https://www.gw-openscience.org/O2/.
[21] Vallisneri M, Kanner J, Williams R, Weinstein A, Stephens B. The LIGO open science center. J Phys Conf Ser 2015;610:012021, arXiv:1410.4839.
[22] Green MA, Moffat JW. Extraction of black hole coalescence waveforms from noisy data. Phys Lett B 2018;784:312, arXiv:1711.00347.
[23] Nielsen AB, Nitz AH, Capano CD, Brown DA. Investigating the noise residuals around the gravitational wave event GW150914. J Cosmol Astropart Phys 2019;1902:019, arXiv:1811.04071.
[24] Nitz AH, et al. 1-OGC: The first open gravitational-wave catalog of binary mergers from analysis of public Advanced LIGO data. Astrophys J 2019;872:195, arXiv:1811.01921.
[25] Zackay B, Venumadhav T, Dai L, Roulet J, Zaldarriaga M. A highly spinning and aligned binary black hole merger in the Advanced LIGO first observing run. Phys Rev D 2019;100:023007, arXiv:1902.10331.
[26] Venumadhav T, Zackay B, Roulet J, Dai L, Zaldarriaga M. New binary black hole mergers in the second observing run of Advanced LIGO and Advanced Virgo. Phys Rev D 2020;101:083030, arXiv:1904.07214.
[27] Nitz AH, et al. 2-OGC: Open gravitational-wave catalog of binary mergers from analysis of public Advanced LIGO and Virgo data, 891. 2020, p. 123, Preprint at https://arxiv.org/abs/1910.05331.
[28] Zackay B, Dai L, Venumadhav T, Roulet J, Zaldarriaga M. Detecting gravitational waves with disparate detector responses: Two new binary black hole mergers. 2019, Preprint at https://arxiv.org/abs/1910.09528.
[29] Kanner JB, et al. Leveraging waveform complexity for confident detection of gravitational waves. Phys Rev D 2016;93:022002, URL https://link.aps.org/doi/10.1103/PhysRevD.93.022002.
[30] Yamamoto T, Hayama K, Mano S, Itoh Y, Kanda N. Characterization of non-gaussianity in gravitational wave detector noise. Phys Rev D 2016;93:082005, URL https://link.aps.org/doi/10.1103/PhysRevD.93.082005.
[31] Green MA, Moffat J. Extraction of black hole coalescence waveforms from noisy data. Phys Lett B 2018;784:312–23, URL http://www.sciencedirect.com/science/article/pii/S0370269318306129.
[32] Gayathri V, et al. Astrophysical signal consistency test adapted for gravitational-wave transient searches. Phys Rev D 2019;100:124022, URL https://link.aps.org/doi/10.1103/PhysRevD.100.124022.
[33] Yanagisawa K, et al. A time–frequency analysis of gravitational wave signals with non-harmonic analysis. Prog Theor Exp Phys 2019;2019:063F01. http://dx.doi.org/10.1093/ptep/ptz043, https://academic.oup.com/ptep/article-pdf/2019/6/063F01/28788035/ptz043.pdf.
[34] Gadre B, Mitra S, Dhurandhar S. Hierarchical search strategy for the efficient detection of gravitational waves from nonprecessing coalescing compact binaries with aligned-spins. Phys Rev D 2019;99:124035, URL https://link.aps.org/doi/10.1103/PhysRevD.99.124035.
[35] Dai L, Venumadhav T, Zackay B. Parameter estimation for GW170817 using relative binning. 2018, Preprint at https://arxiv.org/abs/1806.08793.
[36] De S, Capano CD, Biwer CM, Nitz AH, Brown DA. Posterior samples of the parameters of binary black holes from Advanced LIGO, Virgo's second observing run. Sci Data 2019;6:81, arXiv:1811.09232.
[37] Gerosa D, Vitale S, Haster C-J, Chatziioannou K, Zimmerman A. Reanalysis of ligo black-hole coalescences with alternative prior assumptions. Proc Int Astron Union 2017;13:22–8.
[38] Chatziioannou K, et al. Noise spectral estimation methods and their impact on gravitational wave measurement of compact binary mergers. Phys Rev D 2019;100:104004, URL https://link.aps.org/doi/10.1103/PhysRevD.100.104004.
[39] Kumar P, et al. Constraining the parameters of gw150914 and gw170104 with numerical relativity surrogates. Phys Rev D 2019;99:124005, URL https://link.aps.org/doi/10.1103/PhysRevD.99.124005.
[40] Chatziioannou K, et al. On the properties of the massive binary black hole merger gw170729. Phys Rev D 2019;100:104015, URL https://link.aps.org/doi/10.1103/PhysRevD.100.104015.
[41] Kalaghatgi C, Hannam M, Raymond V. Parameter estimation with a spinning multimode waveform model. Phys Rev D 2020;101:103004, URL https://link.aps.org/doi/10.1103/PhysRevD.101.103004.
[42] Buscicchio R, Roebber E, Goldstein JM, Moore CJ. Label switching problem in bayesian analysis for gravitational wave astronomy. Phys Rev D 2019;100:084041, URL https://link.aps.org/doi/10.1103/PhysRevD.100.084041.
[43] De S, et al. Tidal deformabilities and radii of neutron stars from the observation of GW170817. Phys Rev Lett 2018;121:091102, arXiv:1804.08583.
[44] Carson Z, Chatziioannou K, Haster C-J, Yagi K, Yunes N. Equation-of-state insensitive relations after gw170817. Phys Rev D 2019;99:083016, URL https://link.aps.org/doi/10.1103/PhysRevD.99.083016.
[45] Reyes S, Brown DA. Constraints on nonlinear tides due to *p-g* mode coupling from the neutron-star merger GW170817. Astrophys J 2020;894:41, 1808.07013.
[46] Pratten G, Schmidt P, Hinderer T. Gravitational-wave asteroseismology with fundamental modes from compact binary inspirals. Nature Commun 2020;11:2553.
[47] Hagihara Y, Era N, Iikawa D, Nishizawa A, Asada H. Constraining extra gravitational wave polarizations with advanced ligo, advanced virgo, and kagra and upper bounds from gw170817. Phys Rev D 2019;100:064010, URL https://link.aps.org/doi/10.1103/PhysRevD.100.064010.
[48] Isi M, Weinstein AJ, Mead C, Pitkin M. Detecting beyond-einstein polarizations of continuous gravitational waves. Phys Rev D 2015;91:082002, URL https://link.aps.org/doi/10.1103/PhysRevD.91.082002.
[49] Carullo G, Del Pozzo W, Veitch J. Observational black hole spectroscopy: A time-domain multimode analysis of gw150914. Phys Rev D 2019;99:123029, URL https://link.aps.org/doi/10.1103/PhysRevD.99.123029.
[50] Isi M, Giesler M, Farr WM, Scheel MA, Teukolsky SA. Testing the no-hair theorem with gw150914. Phys Rev Lett 2019;123:111102, URL https://link.aps.org/doi/10.1103/PhysRevLett.123.111102.
[51] Gebhard TD, Kilbertus N, Harry I, Schölkopf B. Convolutional neural networks: A magic bullet for gravitational-wave detection? Phys Rev D 2019;100:063015, URL https://link.aps.org/doi/10.1103/PhysRevD.100.063015.
[52] Wang H, Wu S, Cao Z, Liu X, Zhu J-Y. Gravitational-wave signal recognition of ligo data by deep learning. Phys Rev D 2020;101:104003, URL https://link.aps.org/doi/10.1103/PhysRevD.101.104003.
[53] Hannuksela OA, et al. Search for gravitational lensing signatures in LIGO-virgo binary black hole events. Astrophys J 2019;874:L2. http://dx.doi.org/10.3847/2041-8213/ab0c0f.
[54] Broadhurst T, M. Diego J, F. Smoot G. Twin ligo/virgo detections of a viable gravitationally-lensed black hole merger. 2019, Preprint at https://arxiv.org/abs/1901.03190.
[55] Radice D, Dai L. Multimessenger parameter estimation of GW170817. Eur Phys J A 2019;55:50, arXiv:1810.12917.
[56] Lousto CO, Healy J. Kicking gravitational wave detectors with recoiling black holes. Phys Rev D 2019;100:104039, URL https://link.aps.org/doi/10.1103/PhysRevD.100.104039.
[57] Finstad D, De S, Brown DA, Berger E, Biwer CM. Measuring the viewing angle of GW170817 with electromagnetic and gravitational waves. Astrophys J 2018;860:L2.
[58] Nicolaou C, Lahav O, Lemos P, Hartley W, Braden J. The impact of peculiar velocities on the estimation of the hubble constant from gravitational wave standard sirens. Mon Not R Astron Soc 2020;495:90–7, https://academic.oup.com/mnras/article-pdf/495/1/90/33216608/staa1120.pdf.
[59] Chen Z-C, Huang Q-G. Distinguishing primordial black holes from astrophysical black holes by einstein telescope and cosmic explorer. J Cosmol Astropart Phys 2020;2020. 039–039.
[60] Kwee P, et al. Stabilized high-power laser system for the gravitational wave detector Advanced LIGO. Opt Express 2012;20:10617–34. http://dx.doi.org/10.1364/OE.20.010617.
[61] Winkelmann L, et al. Injection-locked single-frequency laser with an output power of 220 W. Appl Phys B 2011;102:529–38. http://dx.doi.org/10.1007/s00340-011-4411-9.
[62] Liu Z, et al. Feedback control of optical beam spatial profiles using thermal lensing. Appl Opt 2013;52:6452–7. http://dx.doi.org/10.1364/AO.52.006452.
[63] Palashov OV, et al. High-vacuum-compatible high-power faraday isolators for gravitational-wave interferometers. J Opt Soc Amer B 2012;29:1784–92. http://dx.doi.org/10.1364/JOSAB.29.001784.
[64] Dooley KL, et al. Thermal effects in the input optics of the enhanced laser interferometer gravitational-wave observatory interferometers. Rev Sci Instrum 2012;83. http://dx.doi.org/10.1063/1.3695405.
[65] Arain MA, Mueller G. Design of the Advanced LIGO recycling cavities. Opt Express 2008;16:10018–32, URL http://www.opticsexpress.org/abstract.cfm?URI=oe-16-14-10018.

[66] Mueller CL, et al. The Advanced LIGO input optics. Rev Sci Instrum 2016;87:014502, URL http://scitation.aip.org/content/aip/journal/rsi/87/1/10.1063/1.4936974.
[67] Harry GM, et al. Titania-doped tantala/silica coatings for gravitational-wave detection. Classical Quantum Gravity 2007;24:405, URL http://stacks.iop.org/0264-9381/24/i=2/a=008.
[68] Granata M, et al. Mechanical loss in state-of-the-art amorphous optical coatings. Phys Rev D 2016;93:012007. http://dx.doi.org/10.1103/PhysRevD.93.012007.
[69] Pinard L, et al. Mirrors used in the LIGO interferometers for first detection of gravitational waves. Appl Opt 2017;56:C11. http://dx.doi.org/10.1364/AO.56.000C11.
[70] Abbott BP, et al., LIGO Scientific Collaboration, Virgo Collaboration. GW150914: The Advanced LIGO detectors in the era of first discoveries. Phys Rev Lett 2016;116:131103, URL http://link.aps.org/doi/10.1103/PhysRevLett.116.131103.
[71] Buonanno A, Chen Y. Signal recycled laser-interferometer gravitational-wave detectors as optical springs. Phys Rev D 2002;65:042001, URL https://link.aps.org/doi/10.1103/PhysRevD.65.042001.
[72] Heptonstall A, et al. Enhanced characteristics of fused silica fibers using laser polishing. Classical Quantum Gravity 2014;31:105006, URL http://stacks.iop.org/0264-9381/31/i=10/a=105006.
[73] Bell CJ, et al. Experimental results for nulling the effective thermal expansion coefficient of fused silica fibres under a static stress. Classical Quantum Gravity 2014;31:065010, URL http://stacks.iop.org/0264-9381/31/i=6/a=065010.
[74] Tokmakov K, et al. A study of the fracture mechanisms in pristine silica fibres utilising high speed imaging techniques. J Non Cryst Solids 2012;358:1699–709, URL http://www.sciencedirect.com/science/article/pii/S0022309312002554.
[75] Hammond GD, et al. Reducing the suspension thermal noise of advanced gravitational wave detectors. Classical Quantum Gravity 2012;29:124009, URL http://stacks.iop.org/0264-9381/29/i=12/a=124009.
[76] Aston SM, et al. Update on quadruple suspension design for Advanced LIGO. Classical Quantum Gravity 2012;29:235004, URL http://stacks.iop.org/0264-9381/29/i=23/a=235004.
[77] Carbone L, et al. Sensors and actuators for the Advanced LIGO mirror suspensions. Classical Quantum Gravity 2012;29:115005, URL http://stacks.iop.org/0264-9381/29/i=11/a=115005.
[78] Cumming AV, et al. Design and development of the Advanced LIGO monolithic fused silica suspension. Classical Quantum Gravity 2012;29:035003, URL http://stacks.iop.org/0264-9381/29/i=3/a=035003.
[79] Heptonstall A, et al. Invited article: CO_2 laser production of fused silica fibers for use in interferometric gravitational wave detector mirror suspensions. Rev Sci Instrum 2011;82. URL http://scitation.aip.org/content/aip/journal/rsi/82/1/10.1063/1.3532770.
[80] Shapiro BN, et al. Noise and control decoupling of Advanced LIGO suspensions. Classical Quantum Gravity 2015;32:015004, URL http://stacks.iop.org/0264-9381/32/i=1/a=015004.
[81] Matichard F, et al. ADvanced LIGO two-stage twelve-axis vibration isolation and positioning platform. part 1: Design and production overview. Precis Eng 2015;40:273–86, URL http://www.sciencedirect.com/science/article/pii/S0141635914001561.
[82] Matichard F, et al. ADvanced LIGO two-stage twelve-axis vibration isolation and positioning platform. part 2: Experimental investigation and tests results. Precis Eng 2015;40:287–97, URL http://www.sciencedirect.com/science/article/pii/S0141635914002098.
[83] Matichard F, et al. Seismic isolation of Advanced LIGO: Review of strategy, instrumentation and performance. Classical Quantum Gravity 2015;32:185003, URL http://stacks.iop.org/0264-9381/32/i=18/a=185003.
[84] Wen S, et al. Hydraulic external pre-isolator system for LIGO. Classical Quantum Gravity 2014;31:235001, URL http://stacks.iop.org/0264-9381/31/i=23/a=235001.
[85] Daw EJ, Giaime JA, Lormand D, Lubinski M, Zweizig J. Long-term study of the seismic environment at LIGO. Classical Quantum Gravity 2004;21:2255, URL http://stacks.iop.org/0264-9381/21/i=9/a=003.
[86] Barsotti L, Evans M, Fritschel P. Alignment sensing and control in Advanced LIGO. Classical Quantum Gravity 2010;27:084026, URL http://stacks.iop.org/0264-9381/27/i=8/a=084026.
[87] Staley A, et al. High precision optical cavity length and width measurements using double modulation. Opt Express 2015;23:19417–31, URL http://www.opticsexpress.org/abstract.cfm?URI=oe-23-15-19417.
[88] Evans M, et al. Observation of parametric instability in Advanced LIGO. Phys Rev Lett 2015;114:161102, URL http://link.aps.org/doi/10.1103/PhysRevLett.114.161102.
[89] Rollins JG. Distributed state machine supervision for long-baseline gravitational-wave detectors. Rev Sci Instrum 2016;87. URL http://scitation.aip.org/content/aip/journal/rsi/87/9/10.1063/1.4961665.
[90] Phelps MH, Gushwa KE, Torrie CI. Optical contamination control in the Advanced LIGO ultra-high vacuum system. Proc SPIE 2013;8885:88852E. http://dx.doi.org/10.1117/12.2047327.
[91] Smith MR. Scattered light control in Advanced LIGO. World Scientific Publishing Company; 2012, URL http://www.worldscientific.com/doi/abs/10.1142/9789814374552_0312.
[92] Brooks AF, et al. Direct measurement of absorption-induced wavefront distortion in high optical power systems. Appl Opt 2009;48:355–64, URL http://ao.osa.org/abstract.cfm?URI=ao-48-2-355.
[93] Lawrence R, Zucker M, Fritschel P, Marfuta P, Shoemaker D. Adaptive thermal compensation of test masses in Advanced LIGO. Classical Quantum Gravity 2002;19:1803, URL http://stacks.iop.org/0264-9381/19/i=7/a=377.
[94] Heitmann H, on behalf of the Virgo Collaboration. Status of the Advanced Virgo gravitational wave detector. Proc SPIE 2018;10700:1070017. http://dx.doi.org/10.1117/12.2312572.
[95] Granata M, et al. Amorphous optical coatings of present gravitational-wave interferometers. 2019, Preprint at https://arxiv.org/abs/1909.03737.
[96] Amato A, et al. Optical properties of high-quality oxide coating materials used in gravitational-wave advanced detectors. J Phys Mater 2019;2:035004.
[97] Bersanetti D, et al. New algorithm for the guided lock technique for a high-finesse optical cavity. Astropart Phys 2020;117:102405, URL https://doi.org/10.1016/j.astropartphys.2019.102405.
[98] Acernese F, et al., Virgo Collaboration. The advanced Virgo longitudinal control system for the O2 observing run. Astropart Phys 2020;116:102386, URL https://doi.org/10.1016/j.astropartphys.2019.07.005.
[99] Aiello L, et al. Thermal compensation system in advanced and third generation gravitational wave interferometric detectors. J Phys Conf Ser 2019;1226:012019.
[100] Cirone A, et al. Investigation of magnetic noise in Advanced Virgo. Classical Quantum Gravity 2019;36:225004, Preprint at https://arxiv.org/abs/1908.11174.
[101] Cirone A, et al. Magnetic coupling to the Advanced Virgo payloads and its impact on the low frequency sensitivity. Rev Sci Instrum 2018;89:114501. http://dx.doi.org/10.1063/1.5045397.
[102] Tringali MC, et al. Seismic array measurements at Virgo's west end building for the configuration of a Newtonian-noise cancellation system. Classical Quantum Gravity 2019. URL http://iopscience.iop.org/10.1088/1361-6382/ab5c43.
[103] van Heijningen JV, et al. A multistage vibration isolation system for Advanced Virgo suspended optical benches. Classical Quantum Gravity 2019;36:075007.
[104] Staley A, et al. Achieving resonance in the advanced LIGO gravitational-wave interferometer. Classical Quantum Gravity 2014;31:245010. http://dx.doi.org/10.1088/0264-9381/31/24/245010.
[105] Abbott BP, et al., LIGO Scientific Collaboration, Virgo Collaboration. Characterization of transient noise in Advanced LIGO relevant to gravitational wave signal GW150914. Classical Quantum Gravity 2016;33:134001, arXiv:1602.03844.
[106] Effler A, et al. Environmental influences on the LIGO gravitational wave detectors during the 6th science run. Classical Quantum Gravity 2015;32:035017.
[107] Finn LS, Chernoff DF. Observing binary inspiral in gravitational radiation: One interferometer. Phys Rev D 1993;47:2198–219, arXiv:gr-qc/9301003.
[108] Chen H-Y, et al. Distance measures in gravitational-wave astrophysics and cosmology. 2017, arXiv:1709.08079.
[109] Abbott BP, et al., LIGO Scientific Collaboration, Virgo Collaboration. Low-latency gravitational-wave alerts for multimessenger astronomy during the second Advanced LIGO and virgo observing run. Astrophys J 2019;875:161.
[110] Abbott BP, et al., LIGO Scientific Collaboration, Virgo Collaboration. Search for intermediate mass black hole binaries in the first and second observing runs of the Advanced LIGO and virgo network. Phys Rev D 2019;100:064064.
[111] Bartos I, et al. The Advanced LIGO timing system. Classical Quantum Gravity 2010;27:084025, URL http://stacks.iop.org/0264-9381/27/i=8/a=084025.
[112] Goetz E, Savage RL. Calibration of the LIGO displacement actuators via laser frequency modulation. Classical Quantum Gravity 2010;27:215001. http://dx.doi.org/10.1088/0264-9381/27/21/215001.
[113] Goetz E, et al. Accurate calibration of test mass displacement in the LIGO interferometers. Classical Quantum Gravity 2010;27:084024, URL http://stacks.iop.org/0264-9381/27/i=8/a=084024.
[114] Goetz E, et al. Precise calibration of LIGO test mass actuators using photon radiation pressure. Classical Quantum Gravity 2009;26:245011, URL http://stacks.iop.org/0264-9381/26/i=24/a=245011.
[115] Abadie J, et al., LIGO Scientific Collaboration. Calibration of the LIGO gravitational wave detectors in the fifth science run. Nucl Instrum Methods Phys Res A 2010;624:223–40, URL http://www.sciencedirect.com/science/article/pii/S0168900210017031.

[116] Accadia T, et al., Virgo Collaboration. Reconstruction of the gravitational wave signal h(t) during the Virgo science runs and independent validation with a photon calibrator. Classical Quantum Gravity 2014;31:165013.
[117] Accadia T, et al., Virgo Collaboration. Calibration and sensitivity of the virgo detector during its second science run. Classical Quantum Gravity 2010;28:025005.
[118] Viets AD, et al. Reconstructing the calibrated strain signal in the Advanced LIGO detectors. Classical Quantum Gravity 2018;35:095015, arXiv:1710.09973.
[119] Acernese F, et al., Virgo Collaboration. Calibration of Advanced Virgo and reconstruction of the gravitational wave signal $h(t)$ during the observing run O2. Classical Quantum Gravity 2018;35:205004.
[120] Cahillane C, et al. Calibration uncertainty for Advanced LIGO's first and second observing runs. Phys Rev D 2017;96:102001, arXiv:1708.03023.
[121] Abbott BP, et al., LIGO Scientific Collaboration. Calibration of the Advanced LIGO detectors for the discovery of the binary black-hole merger GW150914. Phys Rev D 2017;95:062003, URL https://link.aps.org/doi/10.1103/PhysRevD.95.062003.
[122] LIGO Scientific Collaboration and Virgo Collaboration. LIGO/Virgo public alerts user guide. 2018, URL https://emfollow.docs.ligo.org/userguide/.
[123] LIGO Scientific Collaboration and Virgo Collaboration. Data release for event GW150914. 2016, URL https://www.gw-openscience.org/events/GW150914/.
[124] LIGO Scientific Collaboration and Virgo Collaboration. Data release for event LVT151012. 2016, URL https://www.gw-openscience.org/events/LVT151012/.
[125] LIGO Scientific Collaboration and Virgo Collaboration. Data release for event GW151226. 2016, URL https://www.gw-openscience.org/events/GW151226/.
[126] LIGO Scientific Collaboration and Virgo Collaboration. Data release for event GW170104. 2017, URL https://www.gw-openscience.org/events/GW170104/.
[127] LIGO Scientific Collaboration and Virgo Collaboration. Data release for event GW170608. 2017, URL https://www.gw-openscience.org/events/GW170608/.
[128] LIGO Scientific Collaboration and Virgo Collaboration. Data release for event GW170814. 2017, URL https://www.gw-openscience.org/events/GW170814/.
[129] LIGO Scientific Collaboration and Virgo Collaboration. Data release for event GW170817. 2017, URL https://www.gw-openscience.org/events/GW170817/.
[130] Martynov DV, et al. Sensitivity of the Advanced LIGO detectors at the beginning of gravitational wave astronomy. Phys Rev D 2016;93:112004, URL https://link.aps.org/doi/10.1103/PhysRevD.93.112004.
[131] Adhikari R. Sensitivity and noise analysis of 4 km laser interferometric gravitational wave antennae [Ph.D. thesis], Massachusetts Institute of Technology; 2004.
[132] Abbott BP, et al., LIGO Scientific Collaboration, Virgo Collaboration. A guide to LIGO-virgo detector noise and extraction of transient gravitational-wave signals. 2019, Preprint at https://arxiv.org/abs/1908.11170.
[133] Covas PB, et al. Identification and mitigation of narrow spectral artifacts that degrade searches for persistent gravitational waves in the first two observing runs of Advanced LIGO. Phys Rev D 2018;97:082002, arXiv:1801.07204.
[134] Fiori I. O2 lines summary. 2017, URL https://logbook.virgo-gw.eu/virgo/?r=40306.
[135] Aasi J, et al. The characterization of virgo data and its impact on gravitational-wave searches. Classical Quantum Gravity 2012;29:155002, 1203.5613.
[136] Abbott BP, et al., LIGO Scientific Collaboration, Virgo Collaboration. Effects of data quality vetoes on a search for compact binary coalescences in Advanced LIGO's first observing run. Classical Quantum Gravity 2018;35:065010, arXiv:1710.02185.
[137] Davis D, et al. Improving the sensitivity of Advanced LIGO using noise subtraction. Classical Quantum Gravity 2019;36:055011, arXiv:1809.05348.
[138] Pankow C, et al. Mitigation of the instrumental noise transient in gravitational-wave data surrounding GW170817. Phys Rev D 2018;98:084016, URL https://link.aps.org/doi/10.1103/PhysRevD.98.084016.
[139] Biwer C, et al. Validating gravitational-wave detections: The Advanced LIGO hardware injection system. Phys Rev D 2017;95:062002, arXiv:1612.07864.
[140] URL https://cernvm.cern.ch/fs/.
[141] Weitzel D, et al. Data access for LIGO on the OSG. In: Proceedings of the practice and experience in advanced research computing 2017 on sustainability, success and impact; 2017.
[142] Ellis G. Control system design guide. 4th ed. Butterworth-Heinemann; 2012.
[143] Jones E, et al. SciPy: Open source scientific tools for Python. 2001, URL http://www.scipy.org/.
[144] Nyquist H. Certain factors affecting telegraph speed. Bell Syst Tech J 1924;3:324–46.
[145] Nyquist H. Certain topics in telegraph transmission theory. Trans AIEE 1928;47:617–44.
[146] Shannon CE. Communication in the presence of noise. Proc IRE 1949;37:10–21.
[147] Koziol Q, Robinson D. HDF5. 2018, http://dx.doi.org/10.11578/dc.20180330.1.
[148] LIGO Scientific Collaboration and Virgo Collaboration. Specification of a common data frame format for interferometric gravitational wave detectors. Tech. rep. VIR-067A-08, 2009, URL https://dcc.ligo.org/LIGO-T970130/public.
[149] Nitz AH, et al. PyCBC software. GitHub repository; 2017, URL https://github.com/ligo-cbc/pycbc.
[150] Usman SA, et al. The PyCBC search for gravitational waves from compact binary coalescence. Classical Quantum Gravity 2016;33:215004, arXiv:1508.02357.
[151] Sachdev S, et al. The GstLAL search analysis methods for compact binary mergers in Advanced LIGO's second and Advanced Virgo's first observing runs. Phys Rev D 2019 [submitted for publication]. Preprint at https://arxiv.org/abs/1901.08580.
[152] Cody M, et al. Analysis framework for the prompt discovery of compact binary mergers in gravitational-wave data. Phys Rev D 2017;95:042001, arXiv:1604.04324.
[153] Abbott BP, et al., LIGO Scientific Collaboration, Virgo Collaboration. Search for subsolar mass ultracompact binaries in Advanced LIGO's second observing run. Phys Rev Lett 2019;123:161102.
[154] Klimenko S, et al. Method for detection and reconstruction of gravitational wave transients with networks of advanced detectors. Phys Rev D 2016;93:042004, arXiv:1511.05999.
[155] Abbott BP, et al., LIGO Scientific Collaboration, Virgo Collaboration. All-sky search for short gravitational-wave bursts in the second Advanced LIGO and Advanced Virgo run. Phys Rev D 2019;100:024017.
[156] Abbott BP, et al., LIGO Scientific Collaboration, Virgo Collaboration. An optically targeted search for gravitational waves emitted by core-collapse Supernovae during the first and second observing runs of Advanced LIGO and Advanced Virgo. 2019, Preprint at https://arxiv.org/abs/1908.03584.
[157] Lynch R, Vitale S, Essick R, Katsavounidis E, Robinet F. Information-theoretic approach to the gravitational-wave burst detection problem. Phys Rev D 2017;95:104046.
[158] Littenberg TB, Kanner JB, Cornish NJ, Millhouse M. Enabling high confidence detections of gravitational-wave bursts. Phys Rev D 2016;94:044050.
[159] Abbott BP, et al., LIGO Scientific Collaboration, Virgo Collaboration. All-sky search for continuous gravitational waves from isolated neutron stars using Advanced LIGO O2 data. Phys Rev D 2019;100:061101, URL https://link.aps.org/doi/10.1103/PhysRevD.100.024004.
[160] Abbott BP, et al., LIGO Scientific Collaboration, Virgo Collaboration. Narrow-band search for gravitational waves from known pulsars using the second LIGO observing run. Phys Rev D 2019;99:122002, URL https://link.aps.org/doi/10.1103/PhysRevD.99.122002.
[161] Abbott BP, et al., LIGO Scientific Collaboration, Virgo Collaboration. Searches for gravitational waves from known pulsars at two harmonics in 2015–2017 LIGO data. Astrophys J 2015;879:10.
[162] Search for gravitational waves from scorpius X-1 in the first Advanced LIGO observing run with a hidden Markov model. Phys Rev D 2017;95:122003.
[163] Abbott BP, et al., LIGO Scientific Collaboration, Virgo Collaboration. Upper limits on the stochastic gravitational-wave background from Advanced LIGO's first observing run. Phys Rev Lett 2017;118:121101, URL https://link.aps.org/doi/10.1103/PhysRevLett.118.121101.
[164] Abbott BP, et al., LIGO Scientific Collaboration, Virgo Collaboration. Search for the isotropic stochastic background using data from Advanced LIGO's second observing run. Phys Rev D 2019;100:061101, URL https://link.aps.org/doi/10.1103/PhysRevD.100.061101.
[165] LIGO Scientific Collaboration and Virgo Collaboration. H1 lines cleaning file for O1 - version 3. 2015, URL https://www.gw-openscience.org/static/speclines/o1/O1LinesToBeCleaned_H1_v3.txt.
[166] LIGO Scientific Collaboration and Virgo Collaboration. L1 lines cleaning file for O1 - version 3. 2015, URL https://www.gw-openscience.org/static/speclines/o1/O1LinesToBeCleaned_L1_v3.txt.
[167] LIGO Scientific Collaboration and Virgo Collaboration. H1 lines cleaning file for O2 - version 2. 2019, URL https://www.gw-openscience.org/static/speclines/o2/O2LinesToBeCleaned_H1_v2.txt.
[168] LIGO Scientific Collaboration and Virgo Collaboration. L1 lines cleaning file for O2 - version 2. 2019, URL https://www.gw-openscience.org/static/speclines/o2/O2LinesToBeCleaned_L1_v2.txt.

[169] LIGO Scientific Collaboration and Virgo Collaboration. List of lines for Virgo V1 during O2 - 20190209, version 1. 2019, URL https://www.gw-openscience.org/static/speclines/o2/O2_lines_Virgo_V1.txt.
[170] LIGO Scientific Collaboration and Virgo Collaboration. Data quality vetoes applied to the analysis of GW150914. 2016, https://dcc.ligo.org/public/0123/T1600011/003/DQdoc.pdf.
[171] Kluyver T, et al. Jupyter notebooks – a publishing format for reproducible computational workflows. In: Positioning and power in academic publishing: Players, agents and agendas. IOS Press; 2016, p. 87–90.
[172] LIGO Scientific Collaboration. Source code for: LIGO algorithm library - LALSuite. 2018, http://dx.doi.org/10.7935/GT1W-FZ16.
[173] Macleod D, et al. Source code for: GWpy software. 2019, http://dx.doi.org/10.5281/zenodo.2603187.
[174] Home page for: GstLAL – https://wiki.ligo.org/Computing/DASWG/GstLAL.
[175] Ashton G, et al. BILBY: A user-friendly Bayesian inference library for gravitational-wave astronomy. Astrophys J Suppl Ser 2019;241:27. http://dx.doi.org/10.5281/zenodo.2602178.
[176] Veitch J, et al. Parameter estimation for compact binaries with ground-based gravitational-wave observations using the lalinference software library. Phys Rev D 2015;91:042003.
[177] J. Cornish N, Littenberg TB. Bayeswave: Bayesian inference for gravitational wave bursts and instrument glitches. Classical Quantum Gravity 2015;32:135012, arXiv:1410.3835.
[178] Littenberg TB, Cornish NJ. Bayesian inference for spectral estimation of gravitational wave detector noise. Phys Rev D 2015;91:084034.
[179] Gravitational wave open science center (GWOSC). http://www.gw-openscience.org.
[180] GWTC-1: A gravitational-wave transient catalog of compact binary mergers observed by LIGO and Virgo during the first and second observing runs. 2018, http://dx.doi.org/10.7935/82H3-HH23, URL https://dcc.ligo.org/LIGO-P1800307/public.
[181] How to acknowledge use of LIGO/Virgo data through GWOSC. https://www.gw-openscience.org/acknowledgement/.